University of Latvia
Faculty of Physics and Mathematics

The study of nuclear shape phase transitions and quantum chaos in the frameworks of geometrical and algebraic models of even-even nuclei

Jevgenijs Proskurins

Dissertation's resume

Work performed
in the Nuclear Reaction Laboratory
Institute of Solid State Physics
University of Latvia

Scientific advisor
Dr.phys. Tamara Krasta

Riga, 2010

Abstract

This resume of a physics doctor dissertation is devoted to the use of quantum phase transition and chaos conceptions in algebraic and geometrical nuclear structure models. In the frameworks of algebraic approach of the standard Interacting Boson model (IBM-1), nuclear shape phase transitions are studied employing corresponding classical energy functional expressions depending on nuclear quadrupole deformation parameters β and γ. Model parameter values, corresponding to phase transition critical lines and points, are obtained via a precise solution of equations for minima conditions. The results are compared with those obtained using the Landau method of the energy functional expansion in Taylor series. The above analysis of nuclear shape phase transitions is performed in the case of simplified Casten's version of IBM-1, in the case of $O(6)$-limit IBM-1 Hamiltonian including three-boson interaction terms, and in the case of complete IBM-1 Hamiltonian. Behaviour of quantum chaos statistical criteria - the nearest level energy spacing distribution $P(S)$, and dynamical criteria - the entropy of perturbed Hamiltonian H state wave functions $W(\Psi_i)$, and the fragmentation width of unperturbed Hamiltonian H_0 state basis functions $\kappa(\Phi_k)$, is studied in dependence from nuclear shape parameters in the frameworks of algebraic (simplified Casten's version of IBM-1) and geometrical (rigid triaxial rotator) models. Especial attention is given to model parameter ranges in the vicinity of nuclear shape phase transition critical lines and points. The developed methods are applied for the analysis of critical phenomena experimentally observed in the structure of tungsten, osmium, and platinum even-even nuclei with $184 \leq A \leq 194$ belonging to the $A \sim 190$ region.

The results of dissertation have been published in three refereed journal papers, and one paper in international conference proceedings book; additional two journal papers have been submitted for publication. One journal paper has been published in the local scientific journal. The results of dissertation have been reported in eight oral and two poster presentations both at international and local scientific conferences. The Bibliography of the full dissertation text includes 63 titles.

1 Introduction

Progress in the development of experimental techniques allowing to study nuclei far from stability region and at high spin values, as well as extensive use of nuclear models based on group theory approach spurted, especially during last two decades, an interest in the study of critical phenomena in nuclear structure. Scientific literature on nuclear physics includes a great number of papers devoted to various aspects of quantum phase transitions (QPT) and quantum chaos (see, e.g., a most extensive review article of P.Cejnar and J.Jolie [1], and references therein). In these studies, nuclear theoreticians apply conceptions and methods developed for other physical systems: e.g., for the study of QPT in nuclei, the classical thermodynamics approach is used, including the Landau theory of phase transitions.

Algebraic models allow one to present system's Hamiltonian in terms of Casimir invariants belonging to some integrable (regular) system, which enables one to perform numerical analysis of phase transitions in terms of chosen critical variables. The most popular of these algebraic nuclear models is the standard interacting boson model IBM-1, and its simplified two-parametric Casten's version employed for quantum chaos, and QPT studies by most of authors.

Historically first most important results about quantum chaos, and QPT relationships in the frameworks of IBM-1 were published in papers by Y. Alhassid et al. [2, 3]. They studied chaos in the properties (energies, and E2 transitions) of low-lying collective states of even-even nuclei introducing a simplified two-parametric IBM-1 Hamiltonian. The use of such approach allowed to study transitions between three limiting cases of IBM-1 via a change of one chosen variable. These studies were developed further by P. Cejnar, J. Jolie, and co-workers in [4, 5, 6, 7]. In [4], the information entropy of IBM-1 wave functions with respect to dynamical symmetry limits has been proposed as a measure of a symmetry breaking, i.e. a transition from one type of system's symmetry to another. Relationships between shape phase transitions and wave function entropy have been analyzed employing the classical energy functional expression of simplified Casten's version of IBM-1.

A somewhat different approach to the analysis of QPT in the complete version of IBM-1 has been proposed by E. López-Moreno and O. Castaños [8]. They have employed for the analysis of E_{cl} energy surfaces the formalism of the catastrophe theory and have shown that the equilibrium configurations, in the most general case, can be classified employing just two essential control variables (r_1, r_2) that are derived from the parameters of the complete IBM-1 Hamiltonian.

However, there always is a possibility that some previously uncleared details, both theoretical and experimental, would lead to a deeper understanding of certain phenomena. Therefore, we have undertaken a study in the field seemingly well-covered by publications - the QPT and quantum chaos in algebraic (IBM-1) and geometrical (rigid triaxial rotator) nuclear models. There still are some unanswered questions that we shall try to answer. One of these questions is the extent to which a use of thermodynamics methods is justified in the case of nuclear theory, when the number of constituent particles is limited. Therefore, we shall consider an approach alternative to the ordinarily used Landau theory of phase transitions. When studying quantum chaos, the usually considered criteria are the energy level spacing distribution, and the wave function entropy. We shall try to show that the fragmentation width of basis states [9], which is widely used in reaction theory, can be successfully applied as a quantum chaos criterion for nuclear structure models. Developed theoretical methods of QPT and quantum chaos studies will be applied for the analysis of experimentally observed critical phenomena in the structure of even-even nuclei belonging to the transitional deformation region at $A \sim 190$, studied by the physicists of the LU ISSP Nuclear Reaction Laboratory.

Also, the understanding of such fundamental concepts as the quantum system's phase transitions, and the relationship between system's symmetries and quantum chaos, as well as the use of these conceptions for the study of a complex physical object - an atomic nucleus, have a considerable methodological and educational value. Therefore, the presented physics doctor dissertation serves also as a personal training ground, and a basis for further studies of more complex and actual problems of nuclear physics or any other quantum system's theory.

1.1 Basic conceptions about nuclear shape phase transitions and quantum chaos

In the frameworks of the unified model approach, a nuclear core is described as a drop of incompressible "nuclear liquid". Valence nucleons are moving in the mean field formed by the core that can have spherical or deformed shapes in the equilibrium ground state. One can describe collective excitations of the nuclear core employing collective variables $\alpha_{\lambda\mu}$, defined by the deviation of nuclear surface from the spherical equilibrium shape [10]:

$$R(\theta,\phi,t) = R_0\left[1+\sum_{\lambda\mu}(-1)^{\mu}\alpha_{\lambda-\mu}(t)Y_{\lambda\mu}(\theta,\phi)\right], \tag{1}$$

where R_0 is the radius of the equivalent volume sphere. In the case of quadrupole deformation ($\lambda = 2$), the shape of nucleus in the internal reference frame is characterized by two variables β, and γ; nuclear shape is prolate when $\beta > 0$, and oblate when $\beta < 0$. The asymmetry parameter γ indicates a deviation of the nuclear core from the axial symmetry: when γ=0°, 60°,. . . , the core is axially-symmetric.

In Bohr-Mottelson approach [11], one considers collective excitations of the axially-deformed core – rotation and vibrations, which are the cause of dynamical deformation. These excitations are coupled with single-particle degrees of freedom of valence nucleons. The geometrical approach has been especially successful in the case of deformed nuclei with mass numbers $140 < A < 200$.

Another geometrical model has been proposed in 1958 by A.S. Davydov and G.E. Filippov [12]. They assumed that there are nuclei having a non-axial ground state deformation – rigid triaxial rotators. In such a case, collective coordinates a_0, a_2 assume fixed non-zero values, and nuclear core has three different moments of inertia. Collective nuclear Hamiltonian of an even-even nucleus in the case of rigid triaxial rotator model H^{3ax} can be presented (see, e.g., [10]) as the Hamiltonian of the axially-symmetric rotator H_0^{ax} plus perturbation term, and the matrices of H^{3ax} are diagonalized in the basis of axially-symmetric rotator eigenfunctions. The nuclear triaxial rotator model is interesting for quantum chaos studies because of its relationship to the classical integrable system - the rigid asymmetric top (see, e.g., [13, 14]).

Another phenomenological approach to the description of nuclear core is that of interacting boson models (IBM) [15]. The main idea of IBM is that the nuclear core is built from bosons – pairs of coupled nucleons, characterized by definite angular momentum value l. The number of bosons (N_b) usually is associated with the total number of nucleon pairs (particles or holes) outside the nearest closed proton, and neutron shells for the given nucleus ((Z, N)=2,8,20,28,50,82,126). Nuclear collective Hamiltonian includes single boson excitation terms and two-boson interactions. Single-particle degrees of freedom of valence nucleons, included in the case of odd nuclei (the

Interacting Boson-Fermion model (IBFM)), and odd-odd nuclei (the Interacting Boson-Fermion-Fermion model (IBFFM)), usually are the same ones as used in the unified model. Evaluation of interacting boson models is based on group theory approach, employing algebraic techniques of unitary groups and subgroups, characterizing total number of bosonic and fermionic degrees of freedom.

In the simplest version of IBM - the IBM-1 model (or standard IBM), one uses two types of bosons: one s-boson ($l = 0$) and five d-bosons ($l = 2$). The wave functions of IBM-1 Hamiltonian [15, 16] are classified according to the completely symmetric representations $[N_b]$ of group $U(6)$ in any of three chains:

$$U(6) \supset \left\{ \begin{array}{l} U(5) \supset O(5) \supset O(3) \supset O(2) \\ O(6) \supset O(5) \supset O(3) \supset O(2) \\ SU(3) \supset O(3) \supset O(2) \end{array} \right. \tag{2}$$

Employing Casimir operators of corresponding subgroups, one can present the complete IBM-1 Hamiltonian in multipole expansion form proposed by F. Iachello and A. Arima (see, e.g., [15, 17]):

$$\begin{aligned} H_{sd} &= \varepsilon' n_d + \frac{1}{2}\eta(\mathbf{L}\cdot\mathbf{L}) + \frac{1}{2}\kappa(\mathbf{Q}\cdot\mathbf{Q}) - 5\sqrt{7}\omega\left[[\mathbf{d}^+ \times \tilde{\mathbf{d}}]^{(3)} \times [\mathbf{d}^+ \times \tilde{\mathbf{d}}]^{(3)}\right]^{(0)} \\ &+ 15\xi\left[[\mathbf{d}^+ \times \tilde{\mathbf{d}}]^{(4)} \times [\mathbf{d}^+ \times \tilde{\mathbf{d}}]^{(4)}\right]^{(0)}, \end{aligned} \tag{3}$$

where quadrupole moment operator $\mathbf{Q}$ is presented as [18]

$$\mathbf{Q}(\chi) = [\mathbf{d}^+ \times \tilde{\mathbf{s}} + \mathbf{s}^+ \times \tilde{\mathbf{d}}]^{(2)} + \chi[\mathbf{d}^+ \times \tilde{\mathbf{d}}]^{(2)}, \tag{4}$$

and ε', η, κ, ω, ξ, and χ are model parameters.

Energies and wave functions of the complete IBM-1 Hamiltonian Eq. (3) are obtained by its diagonalization in the basis of eigenfunctions of either of three subgroup chains Eq. (2). All three reduction chains are equivalent, and a rank n of the diagonalized matrix is determined by the total number of bosons N_b. Unperturbed Hamiltonians, containing only diagonal terms (Casimir invariants) of corresponding subgroup chain, are known as the $U(5)$, $O(6)$, and $SU(3)$ limits of IBM-1, which are usually associated with vibrational, asymmetric (γ-unstable) rotator, and axially-symmetric rotator nuclear core excitations [15, 16]. The most general and often used IBM-1 Hamiltonian diagonalization basis is that of the spherical $U(5)$ vibrational limit.

A great attention during last decades has been devoted to the study of thermodynamic phase transitions in finite systems, such as Bose-Einstein condensates, atomic clusters, etc. The notion about quantum phase transitions (QPT), for the most part, is related to the study of critical phenomena of interacting quantum objects at zero temperature, when the only possible cause of the onset of disorder are quantum fluctuations. Then, one observes a transition between two distinct types of the ground state wave function (see, e.g., [1]). Such transition between $H(0)$, and $H(1)$ phases is described via the change of perturbing interaction, which one can trace using a dimensionless control variable ρ that is ordinarily normalized to fit into the range $\rho \in [0,1]$:

$$H(\rho) = H_0 + \rho V = (1-\rho)H(0) + \rho H(1). \tag{5}$$

A crossing of the critical point is usually studied in the infinite size limit when the number of particles $\mathcal{N} \to \infty$.

In the case of atomic nuclei, the classical thermodynamic phase transitions are studied at high excitation energies, and/or high rotation frequencies. In the ground state, and at low energy and spin values, one observes the change of the nuclear shape, which is represented by the minima of nuclear collective potential energy expression $V(\beta,\gamma)$ in the (β,γ) phase space diagram (see, e.g., [10]). Then, one can study transitions between prolate $(\beta > 0)$, oblate $(\beta < 0)$, and spherical $(\beta = 0)$ nuclear shapes. The analysis of the potential energy surface minima in dependence on specific nuclear model parameters allows to study the nuclear shape phase transitions employing either the Landau theory of phase transitions [7], or a catastrophe theory approach [8].

The IBM-1, having a comparatively simple structure due to its algebraic symmetry properties, and including explicit dependence on N and Z via the total boson number N_b, provides a possibility to analyze QPT in a wide range of nuclei. One can study these transitions considering the division of complete IBM-1 Hamiltonian into integrable Hamiltonians H_0 of limiting cases: $U(5)$, $O(6)$, and $SU(3)$, and the perturbation terms depending on chosen control parameter values. A deeper insight in the phenomenon of nuclear shape phase transitions one can obtain studying classical energy functional expressions of corresponding algebraic models, obtained in the $N_b \to \infty$ limit (see, e.g., [19]). Once the classical energy functional expression E_{cl} of employed IBM-1 version is known, one can study its behaviour in the nuclear shape diagram (β,γ), linking it with three limiting cases of IBM-1 employing the notions about first and second order QPT (see, e.g., [20]).

The problem of chaos in quantum physics is still a theme of discussions (see, e.g., [21, 9]). Most of authors support a moderate view stating that the term "quantum chaos" denotes the quantum limit of phenomena characteristic to chaotic systems of classical mechanics. The studies in this direction are based mostly on the use of quasi-classical approximations. However, since the quantum mechanics involves the classical one as its particular limiting case, it is impossible to define quantum chaos in a consistent way from the point of view of classical mechanics. Therefore, the second, strictly negative opinion, persists that there is no such thing as quantum chaos. The third group believes that the chaocitity displayed by quantum systems has a purely quantum origin, related with the symmetry properties of integrals of motion (dynamics) of corresponding quantum systems.

In the consideration of QPT, it has been already noted that the only possible cause of the onset of disorder at zero temperatures are quantum fluctuations. Therefore, the phenomena of QPT and quantum chaos are closely related, just as the starting points of their study, i.e., the division of non-integrable model Hamiltonian H into integrable (symmetric) part H_0 and perturbation term V. Solution of the Schrödinger equation for H is obtained via diagonalization of H matrix in the basis of H_0 eigenfunctions Φ_k $(k = 1, \dots, n)$, giving eigenvalues E_i, and eigenfunctions Ψ_i presented as the superposition

$$\Psi_i = \sum_{k=1}^{n} c_{ik} \Phi_k, \tag{6}$$

where c_{ik} are mixing amplitudes.

The most popular statistical criterion of quantum chaos is a distribution $P(S)$ of nearest level spacings $S = E_{i-1} - E_i$. It has been proved [22] that, for regular, completely integrable quantum systems described by non-degenerate Hamiltonians, the level spacing distribution assumes a Poisson form $P_P(S) = \exp(-S)$. On the contrary, level spacings of the quantum analogue of the classically chaotic system (Sinai's billiard) obey Wigner distribution $P_W(S) = (\pi/2) \cdot S \cdot \exp(-\pi S^2/4)$, which is consistent with the Gauss orthogonal ensembles (GOE) statistics of random matrices (see, e.g., [23]). A transition from the regular (integrable) state of the system to the chaotic (non-integrable) one can analyze employing, e.g., the one-parameter Brody distribution [24]:

$$P_B(S) = aS^{\zeta} \exp\left(-bS^{\zeta+1}\right), \tag{7}$$

where $a = (\zeta + 1)b$, and $b = \left\{\Gamma\left(\frac{\zeta+2}{\zeta+1}\right)\right\}^{\zeta+1}$. The form of distribution is determined by the value of Brody parameter ζ: when ζ=0, one obtains Poisson distribution; when ζ=1 - Wigner distribution.

The most popular dynamical quantum chaos criterion is a Shannon information entropy of the wave function defined as follows [4]:

$$W(\Psi_i) = -\sum_{k=1}^{n} |c_{ik}|^2 \cdot \ln\left(|c_{ik}|^2\right), \tag{8}$$

characterizing the admixture of the integrable (regular) Hamiltonian H_0 eigenfunctions Φ_k in the wave function Ψ_i of the perturbed Hamiltonian H. Minimal value of the wave function entropy $W(\Psi_i)^{min} = 0$ corresponds to unmixed state, the wave function of which coincides with one of H_0 eigenfunctions ($\Psi_i = \Phi_k$). The theoretically possible maximal entropy value $W(\Psi_i)^{max} = ln(n)$ corresponds to the case, when the perturbed Hamiltonian H wave function is uniformly spread (fragmented) over all regular Hamiltonian H_0 basis states, i.e., all mixing amplitudes are $|c_{ik}|^2 = 1/n$.

Another dynamical quantum chaos criterion, proposed by V. Bunakov [9], is the fragmentation of basis states $\kappa(\Phi_k)$. Value of this criterion for the k-th basis state Φ_k of some regular Hamiltonian H_0 is defined [9, 25] as the ratio of Φ_k fragmentation width over the states Ψ_i of the perturbed Hamiltonian H ($\Gamma_{spr}(k)$) to the averaged spacing D_0 of the regular system's eigenvalues ε_k:

$$\kappa(\Phi_k) = \Gamma_{spr}(k)/D_0. \tag{9}$$

However, due to condition

$$|c_{i=k,k}|^2 < 0.5, \tag{10}$$

imposed on mixing amplitudes involved in $\kappa(\Phi_k)$ evaluation, one cannot use this criterion in the case of small perturbations. Criterion $\kappa(\Phi_k)$ allows one to characterize the system's dynamical quantum chaos state as: a) a soft chaos case, when $0 < \kappa(\Phi_k) < 1$; b) a hard chaos case, when $\kappa(\Phi_k) \geq 1$. In the classical limit, the fragmentation width of basis states is transformed [9] to the well-known classical characteristics of chaoticity – the Lyapunov's exponent λ.

1.2 The aims and methods of presented research work

The problems that are to be resolved in the scope of this dissertation can be defined as follows:

1) to obtain precise analytical expressions for the classical energy functional E_{cl} minima conditions in terms of nuclear quadrupole deformation parameter β, and to apply the obtained expressions for the analysis of nuclear shape phase transition critical lines and points in the case of several simplified IBM-1 versions, and in the case of complete IBM-1 Hamiltonian, comparing the results with those obtained employing the approach of the Landau theory of phase transitions, when the higher order terms of E_{cl} expansion are disregarded;

2) to analyze and compare the behaviour of statistical and dynamical quantum chaos criteria in terms of nuclear quadrupole deformation parameters, and shape phase transitions in the frameworks of algebraic IBM-1 and geometric rigid triaxial rotator models of even-even nuclei;

3) to assess a possibility to employ the basis state fragmentation width $\kappa(\Phi_k)$ as a dynamical quantum chaos criterion in the case of algebraic (IBM-1) and geometrical (rigid triaxial rotator) nuclear structure models;

4) to apply the developed theoretical approach for the study of prolate-oblate shape phase transition, which is experimentally observed in the tungsten, osmium, and platinum isotope chains belonging to the $A \sim 190$ region.

For the study of precise analytical solutions of the classical energy functional minima problem, and the comparison of obtained results with those obtained by other authors, following IBM-1 versions have been chosen:

a) the simplified two-parameter Casten's version (see, e.g., [2, 4]);

b) the $O(6)$-limit Hamiltonian with included cubic d-boson interaction terms [26, 27];

c) the $O(6)$-limit Hamiltonian with attached cubic quadrupole moment term $[\hat{Q}\hat{Q}\hat{Q}]^{(0)}$ [28] in two variants: the one conserving the dynamical $O(6)$-symmetry, and the $O(6)$-symmetry non-conserving variant; one should note that, in the latter case, the E_{cl} minima problem has not been studied before;

d) the complete IBM-1 version [15].

For all model versions, precise analytical solutions for the E_{cl} minima condition equations in terms of nuclear quadrupole deformation parameter β (at $\gamma = 0$) have been obtained employing the computer program package Mathematica. The behaviour of these minima in dependence on IBM-1 parameter values has been analyzed in terms of QPT critical lines and points. The results of precise solution method have been compared with analogous results obtained using the Landau phase transition theory approach. The effects due to accounting of higher order terms of E_{cl} expansion have been assessed in the case of complete IBM-1 version.

The standard IBM-1 computer program package PHINT by O. Scholten [17] has been used for the diagonalization of IBM-1 model Hamiltonian in order to obtain eigenvalues and eigenfunctions for the evaluation of statistical ($P(S)$), and dynamical ($W(\Psi_i)$ and $\kappa(\Phi_k)$) quantum chaos criteria, as well as for the calculation of theoretical energy values in the case of selected A ~190 region nuclei.

A specially written computer program has been used for the diagonalization of rigid triaxial rotator model Hamiltonian matrices at different nuclear spin I values. Model Hamiltonian matrices have been obtained in dependence on γ, in the case of Davydov's model [29], and γ and β, in the case of Bravin-Fedorov's model [30, 31].

The behaviour of quantum chaos criteria has been studied in the frameworks of:

a) the algebraic simplified Casten's version of IBM-1; and

b) two geometric rigid triaxial (asymmetric) rotator models.

These models have a relatively simple structure, and a small number of model parameters: one parameter γ - in the case of Davydov's model, and two parameters - in the case of Bravin-Fedorov's model and in the case of simplified Casten's version of IBM-1. Parameters of the Casten's version of IBM-1 (η, χ) are directly linked with the nuclear quadrupole deformation parameters β, γ via classical limit energy E_{cl} expressions. It provides an opportunity to compare the behaviour of quantum chaos criteria in the frameworks of both approaches: geometrical and algebraic.

Hamiltonian matrices of both models at each nuclear spin I value have finite rank: $n = n(I)$, in the case of rigid triaxial rotator models, and $n = n(I, N_b)$, in the case of IBM-1. However, one should take into account that, while nuclear spin I values are unlimited in the frameworks of geometrical approach, in the case of IBM-1, boson number N_b determines a cut-off value for the nuclear spin. The existence of an upper limit affects the observed mixing of IBM-1 states at higher spin values.

The developed methods have been applied for the analysis of relationships between shape phase transitions and quantum chaos criteria in the case of selected nuclei. For this purpose, we have chosen 15 even-even isotopes of tungsten ($Z = 74$), osmium ($Z = 76$), and platinum ($Z = 78$) with $184 \leq A \leq 194$, belonging to the transitional deformation region at $A \sim 190$. Nuclei of these three elements are known to have shapes ranging from the stable prolate axial-symmetry (^{184}W) to the asymmetric γ-unstable form (^{194}Pt). This is one of regions where traditionally the prolate-oblate shape phase transition is studied; so, there is a possibility to compare our results both with experimental data, and with results of other model calculations. The confidently established experimental data about excited level energies and electromagnetic properties of considered nuclei have been taken from the ENSDF data compilations [32] with a deadline up to January 2010. Therefore, we have used for our analysis experimental information which is more accurate than that available for the most of earlier studies.

We have limited our calculations with nuclei belonging to the $184 \leq A \leq 194$ region and having boson numbers N_b from 7 to 12, excluding experimentally well-known heavier platinum isotopes. Such choice was motivated: a) by the lack of confident experimental data about heavy tungsten and osmium isotopes in the ENSDF data base; b) by the fact that one needs a sufficient number of basis states for the calculation of quantum chaos criteria; c) by the circumstance that, at $A \geq 194$, when neutron number approaches the closed shell at $N = 126$, it is hard to distinguish which phase transition takes place - the prolate-to-oblate or the deformed-to-spherical.

Analysis of experimental data shows that the nuclear shape phase transition in the W-Os-Pt region has a very complex nature. In fact, two parallel transitions take place: the $SU(3) - O(6) - \overline{SU(3)}$ phase transition from the deformed prolate shape to the deformed oblate shape, and the deformed-to-spherical $O(6) - E(5) - U(5)$ transition. Besides, deformation of the nuclear ground state and that of higher excitations can be different, i.e, there is a possibility of shape coexistence. Therefore, one must vary IBM-1 parameters in the entire model parameter space, not just along some selected phase transition critical line, i.e., one should use the complete version of IBM-1 in multipole representation, which enables one to describe in a uniform way various nuclear shapes, and to study the transition from one shape to another.

Values of IBM-1 model parameters have been obtained via fitting of theoretical spectra to experimental energies of low-lying collective states in the case of each of considered nuclei. In difference from the most of well-known prolate-oblate shape phase transition studies, we have considered in our analysis the entire low-lying spectrum of each nucleus. Usually, only a few lowest levels are taken into account (see, e.g., [33]). The obtained results have been analyzed both in terms of the $SU(3) - O(6) - \overline{SU}(3)$ first order phase transition control variable χ, and employing the catastrophe theory essential control parameters (r_1, r_2), introduced in [8]. The behaviour of the statistical and dynamical quantum chaos criteria, calculated for each nucleus in the frameworks of algebraic complete IBM-1 version, has been studied both in dependence from the phase transition control parameters, and in dependence from nuclear spin I. A possibility to compare the results of algebraic IBM model with the ones obtained using geometrical rigid triaxial rotator approach has been considered.

2 The studies of QPT and quantum chaos employing simplified IBM-1 versions

We have started our studies of nuclear shape quantum phase transitions and quantum chaos with the most simple algebraic model - the two-parametric Casten's version of IBM-1. The results of these studies have been published in two papers [R1,R2], and reported at the international conference in 2005 [A1].

In the frameworks of Casten's version, Hamiltonian of the standard IBM-1 is written in a following simplified form (see, e.g., [2, 4]):

$$H(N_b, \eta, \chi) = \eta \cdot \mathbf{n}_d + \frac{\eta - 1}{N_b} \mathbf{Q}(\chi) \cdot \mathbf{Q}(\chi), \tag{11}$$

depending from the total boson number N_b, and two model parameters η and χ. In Eq. (11), $\mathbf{n}_d$ is the number operator of d-bosons; and the quadrupole operator $\mathbf{Q}(\chi)$ is defined as Eq. (4). This simplified version retains all dynamical symmetries of complete IBM-1 Hamiltonian [4]. Eq. (11) one can obtain from the multipole representation Hamiltonian Eq. (3) by letting $\varepsilon' = \omega = \xi = 0$. Parameters η, and χ can assume values $0 \leq \eta \leq +1$, and $-\sqrt{7}/2 \leq \chi \leq +\sqrt{7}/2$, varying within the space of extended Casten's triangle. This triangle is formed by lines linking the vertex $\chi = 0$, $\eta = +1$, corresponding to spherical $U(5)$ dynamical symmetry limit of IBM-1, with the $\chi = -\sqrt{7}/2$, $\eta = 0$ and $\chi = +\sqrt{7}/2$, $\eta = 0$ vertexes, corresponding to deformed $SU(3)$- and $\overline{SU}(3)$-symmetric prolate and oblate shapes, respectively. The $\chi = \eta = 0$ point corresponds to the $O(6)$ dynamical symmetry of γ-soft (unstable) shape.

The classical energy functional $E_{cl}(N_b, \eta, \chi; \beta)$ of Hamiltonian Eq.(11) has been obtained in [5]. The condition on the second order derivative of E_{cl} (see, e.g., [34]):

$$\frac{d^2 E_{cl}(N_b, \eta, \chi; \beta)}{d\beta^2}\Big|_{\beta=0} = 0, \tag{12}$$

gives equation for critical points separating spherical $\beta = 0$ and deformed $\beta \neq 0$ shapes:

$$2(N_b\eta - A_0(4N_b^2 + \chi^2 - 8)) = 0. \tag{13}$$

Solution of Eq. (13) with respect to parameter η:

$$\eta = (4N_b + \chi^2 - 8)/(5N_b + \chi^2 - 8), \tag{14}$$

defines the second order phase transition line $X(5) - E(5) - \overline{X(5)}$.

Solution of the equation system consisting from Eq. (14) and condition

$$\chi = \pm(\sqrt{7}/2)(\eta - 1) \tag{15}$$

allows one to obtain values $\chi_{X(5)}$, $\eta_{X(5)}$, describing location of the critical point on the $U(5) - SU(3)$ line, characterized by the $X(5)$ dynamical symmetry [35] (analogously for the $\overline{X(5)}$ point). Solution of Eq. (14) at $\chi = 0$ gives position of an isolated triple point $\eta_{E(5)} = (4N_b - 8)/(5N_b - 8)$ where critical lines of the second order phase transition between spherical and deformed shapes meets with first order phase transition line separating prolate ($\beta > 0$) and oblate ($\beta < 0$) deformations. This critical point is characterized by the $E(5)$ symmetry [36]. Therefore, the first order prolate-oblate phase transition line can be denoted as $E(5) - O(6)$.

Usually one applies for the study of nuclear shape phase transitions the approach proposed by Landau, as it has been done, e.g., in [7, 20]. One uses the expansion $(1 + \beta^2)^{-2} = 1 - 2\beta^2 + 3\beta^4 - 4\beta^6 + \cdots$ and rewrites E_{cl} in the form:

$$E_{cl}(N_b, \eta, \chi; \beta) = E_0(\eta) + A_L(N_b, \eta, \chi)\beta^2 + B_L(N_b, \eta, \chi)\beta^3 + C_L(N_b, \eta, \chi)\beta^4 + \cdots. \tag{16}$$

However, it is possible to obtain a precise analytical solution for the energy minimum, which follows from the extreme condition

$$\frac{\partial E_{cl}(N_b, \eta, \chi; \beta)}{\partial \beta} = 0, \tag{17}$$

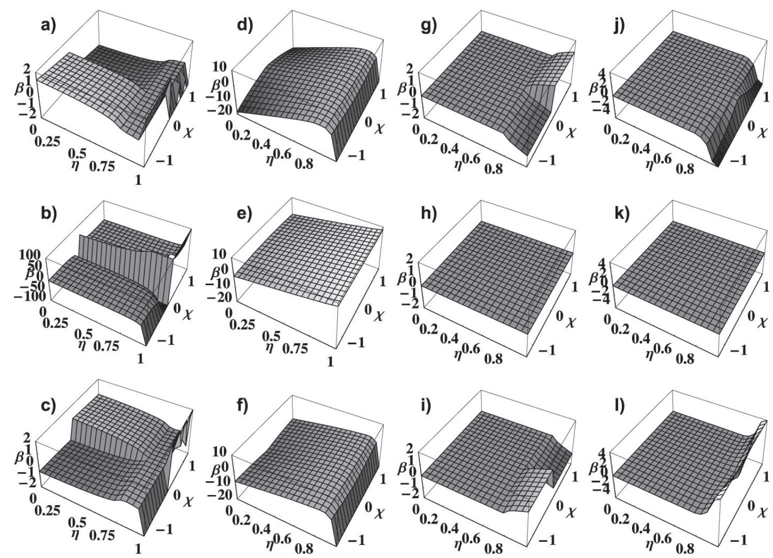

Figure 1: Real (a-c) (and imaginary (g-i)) parts of β_{0i} ($i = 1, 2, 3$), and corresponding minimal energy values $E_{0i}(N_b, \eta, \chi; \beta_{0i})$ (d-f; and j-l). Numerical calculations have been performed at $N_b = 8$.

resulting in cubic equation for nuclear quadrupole deformation parameter β (see [R1, R2]). Solutions of this cubic equation give values of deformation parameter β at the minima of classical energy functional as three roots β_{0i} ($i = 1, 2, 3$), which are complicated and, in general, complex functions from the total boson number N_b and model parameters χ, η.

We have performed the detailed analysis (see [R1,R2]) of the behaviour of cubic equation roots β_{0i} ($i = 1, 2, 3$) in the space of parameters (η, χ) covering the entire extended Casten's triangle. A special attention has been given to regions in the vicinity of phase transition lines and critical points. Similar analysis has been carried out also for corresponding classical energy minimum values $E_0^i = E_0^i(N_b, \chi, \eta; \beta_{0i})$.

In Fig. 1, one can discern clearly the $O(6) - E(5)$ first order phase transition line, separating left and right sides of the extended Casten's triangle (with $\beta_0 > 0$ and $\beta_0 < 0$), as well as the triple point $E(5)$. The roots $\beta_{01,03}$ are real below the $X(5) - E(5) - \overline{X(5)}$ arc line, while the root β_{02} is real in the entire space of Casten's triangle. In the bottom, "deformed shape" part of Casten's triangle, below the $X(5) - E(5) - \overline{X(5)}$ arc line (when $0 \leq \eta \leq \eta(E(5))$), we have three real, unequal roots. However, one of these roots (β_{02}) assumes nonphysically large values. In the top, "spherical shape" part of Casten's triangle, above the arc line $X(5) - E(5) - \overline{X(5)}$ (when $\eta(E(5)) < \eta < 1$), we have one real root (β_{02}) assuming nonphysically large values and two complex conjugate roots (β_{01}, β_{03}), just as one can expect in the spherical shape region.

The results of our approach to the minimum problem of the classical energy functional allow one to obtain precise values of deformation parameter β at each (η, χ) point of Casten's triangle. In general, the qualitative conclusions drawn in our analysis of phase transition critical lines and points in the case of simplified Casten's version of IBM-1 are similar to those obtained employing the Landau theory approach [5, 20]. However, the analytical solution of the classical energy minimum problem allows to obtain more precise numerical values of β_0, and $E_{cl}(N_b, \eta, \chi; \beta_0)$.

Let us consider the results of the evaluation of statistical and dynamical quantum chaos criteria, calculated in selected points within the (η, χ) parameter space represented by Casten's triangle at $N_b = 8$. The number assigned to each point is given in column 1 of Table 1. In the case of $N_b = 8$, the triple point $E(5)$ has coordinates $\eta_{E(5)} = 0.75$, and $\chi = 0$. Values of model parameters have been chosen in the range from below the $X(5) - E(5) - \overline{X(5)}$ second order phase transition line Eq. (14), separating spherical and deformed shapes, to the $SU(3) - O(6) - \overline{SU(3)}$ line (at $\eta = 0$), corresponding to maximal deformation. Calculations have been performed only for the prolate deformation part ($\chi < 0$) of the extended Casten's triangle, since the solutions of IBM-1 Hamiltonian are mirror symmetric with respect to parameter χ values.

The results of statistical quantum chaos criterion calculations show that the simplified Casten's version of IBM-1 at $N_b = 8$ is quite regular. The deviation of nearest level spacings distribution $P(S)$ from the Poisson form is very slight even in the case of maximal mixing farther away from the vertexes of Casten's triangle (see Table 1). The area where one can regularly evaluate both dynamical chaos criteria: $\kappa(\Phi_k)$ and $W(\Psi_i)$, is approximately from the bottom $SU(3) - O(6) - \overline{SU(3)}$ line of the extended Casten's triangle up to about its middle part ($0 < \eta \leq 0.75 \cdot \eta_{E(5)}$), but below the second order phase transition line $X(5) - E(5) - \overline{X(5)}$. Behaviour of dynamical quantum chaos criteria along this phase transition line in shown in Fig. 2.

From the results presented in Table 1, one can see that, on the $U(5) -$

Table 1: Results of quantum chaos criteria calculations in selected points of the Casten's triangle at $N_b = 8$.

Point	χ		η		ζ^a	$\kappa_{av}(\Phi_k)^b$	$W_{av}(\Psi_i)^b$	W_{av}/W^c_{max}
1	χ^d_{max}	-0.5788	$0.75 \cdot \eta^d_{E(5)}$	0.5625	0.157	5.367	1.423	0.618
2	$0.75 \cdot \chi_{max}$	-0.4341	-"-	-"-	-	5.501	1.436	0.624
3	$0.5 \cdot \chi_{max}$	-0.2894	-"-	-"-	0.182	3.028	1.266	0.550
4	$0.25 \cdot \chi_{max}$	-0.1447	-"-	-"-	-	2.765	0.932	0.405
5	$\chi = 0$	0	-"-	-"-	0.170	2.610	-	-
6	χ_{max}	-0.8268	$0.5 \cdot \eta_{E(5)}$	0.3750	0.127	6.516	1.550	0.673
7	$0.75 \cdot \chi_{max}$	-0.6201	-"-	-"-	-	6.137	1.557	0.676
8	$0.5 \cdot \chi_{max}$	-0.4134	-"-	-"-	0.094	7.639	1.562	0.678
9	$0.25 \cdot \chi_{max}$	-0.2067	-"-	-"-	-	4.525	1.276	0.554
10	$\chi = 0$	0	-"-	-"-	0.092	2.750	-	-
11	χ_{max}	-1.0748	$0.25 \cdot \eta_{E(5)}$	0.1875	0.105	7.898	1.786	0.776
12	$0.75 \cdot \chi_{max}$	-0.8061	-"-	-"-	-	6.343	1.712	0.744
13	$0.5 \cdot \chi_{max}$	-0.5374	-"-	-"-	0.124	7.206	1.482	
14	$0.25 \cdot \chi_{max}$	-0.2687	-"-	-"-	-	7.289	1.518	0.644
15	$\chi = 0$	0	-"-	-"-	0.093	1.396	-	-
16	$\chi(SU(3)) = -\sqrt{7}/2$	-1.3229	$\eta = 0$	0	0.061	7.903	1.878	0.816
17	$0.75 \cdot \chi(SU(3))$	-0.9922	-"-	-"-	-	8.806	1.759	0.764
18	$0.5 \cdot \chi(SU(3))$	-0.6614	-"-	-"-	0.115	7.193	1.756	0.763
19	$0.25 \cdot \chi(SU(3))$	-0.3307	-"-	-"-	-	7.649	1.654	0.718
20	$\chi(O(6)) = 0$	0	-"-	-"-	0.012	3.060	-	-

[a] - Brody coefficient value is fitted to $P(S)$ distribution of all n_{lev}=105 theoretical states with L from 0 to $L_{max} = 16$;

[b] - averaged values of dynamical quantum chaos criteria for $L = 0$ states ($n = 10$);

[c] - $W_{max}(\Psi_i) = \ln(10) = 2.302585$;

[d] - χ_{max} value is calculated on the $U(5) - SU(3)$ line as $\chi = -(\sqrt{7}/2)(\eta - 1)$; $\eta_{E(5)}$ – according to expression $\eta_{E(5)} = (4N_b - 8)/(5N_b - 8)$.

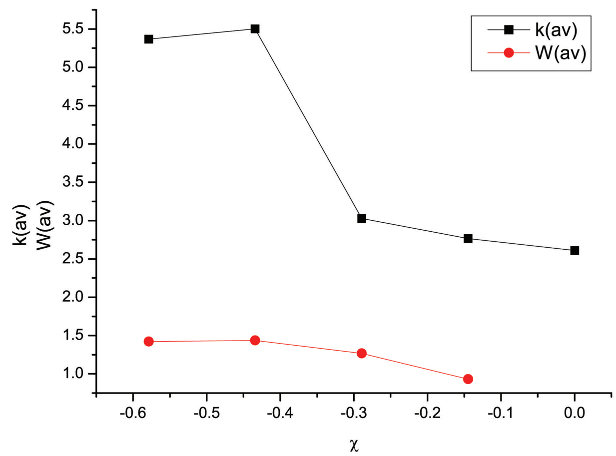

Figure 2: Behaviour of averaged dynamical quantum chaos criteria $\kappa(\Phi_k)_{av}$, and $W(\Psi_i)_{av}$ along the $X(5) - E(5) - \overline{X(5)}$ phase transition line at $N_b = 8$.

$SU(3)$ line and in the area near it (with $\chi = 0.75 \cdot \chi_{max}$), behaviour of $\kappa(\Phi_k)_{av}$ and $W(\Psi_i)_{av}$ values is correlated: increasing from the middle part (with $0.75 \cdot \eta_{E(5)} = 0.5625$) to the bottom line ($\eta = 0$). Correlation between $\kappa(\Phi_k)_{av}$ and $W(\Psi_i)_{av}$ values with respect to parameter χ value, when it is changed in the direction from the $X(5) - SU(3)$ line towards the first order phase transition line $E(5) - O(6)$, is lost when mixing increases.

The studies were continued by considering more complex partial versions of IBM-1, which are obtained when one attaches to the $O(6)$-limit Hamiltonian three-boson interaction terms. Such modification allows one to describe stable triaxial shapes in the frameworks of IBM-1. Phase transitions in the case of $O(6)$-limit Hamiltonians with attached cubic quadrupole moment operator, enabling one to describe rigid rotator $SU(3)$-states attached to a γ-soft core, have been considered as well. The results of our studies have been published in our paper [R3], and reported at the international [A3] and local [A2] scientific conferences in 2006.

It has been shown already in [15] that, in order to obtain stable triaxial shape, one should include into IBM-1 Hamiltonian three-boson interaction terms. This idea has been further developed in [26, 27] where a cubic d-

boson interaction operator H_{3d}, containing terms with $L' = 0, 2, 3, 4, 6$, has been attached to the $O(6)$-limit Hamiltonian of IBM-1, and a corresponding classical energy $E_{3d}(O(6))$ expression has been obtained.

In order to study problems related with the description of stable triaxial shapes when different L' three-boson interaction terms are included, we have analyzed minima of the classical energy expression with respect to quadrupole deformation parameters β and γ employing conditions

$$\frac{\partial E_{3d}(O(6))}{\partial \beta} = \frac{\partial E_{3d}(O(6))}{\partial \gamma} = 0. \tag{18}$$

Analysis of the obtained results [R3] allows to make following conclusions:

1) the cubic d-boson interaction term with $L' = 0$ gives no contribution to the classical energy minimum value $E_{min} = E_{3d}(O(6), \beta_0, \gamma_0 = 30°)$: total classical energy minimum in this case coincides with that of the $O(6)$-limit of IBM-1;

2) in the case of $L' = 2$ term, classical energy contribution from the cubic d-boson interaction does not depend from the asymmetry parameter γ. Therefore, this term cannot be a cause of triaxial shape;

3) the remaining three separate cubic d-boson interaction terms with $L' = 3, 4, 6$ give energy minimum values at $\beta_0 \neq 0$, and $\gamma_0 = 30°$. The same is true also for the case when one includes the sum of all terms with $L' = 0, 2, 3, 4, 6$.

Analysis of the equilibrium deformation β_0 values in dependence from the total boson number N_b, performed in the case of attached separate $L' = 0, 3, 4, 6$ terms, and in the case of all three-boson interaction terms, disclosed following features:

1) in the case of $L' = 0$ term, β_0 values are increasing with growing N_b values: at $N_b \to \infty$, the total classical energy minimum is attained at $\beta_0 = 1$, i.e., one obtains the same result as in the case of pure γ-independent $O(6)$ limit of IBM-1 (see p.108 in [15]);

2) in the case of $L' = 3$ term, the value $N_b = 8$, considered in [27], turns out to be the maximal boson number, at which the energy minimum satisfying conditions Eq.(18) is possible at used parameter values. There is no energy minimum for boson numbers $N_b > 8$.

3) in the case of $L' = 4, 6$ terms, and in the case of sum of all terms, β_0 values are increasing until some maximal β_0^{max} value (at $N_b^{max} = 18, 12, 11$, correspondingly) is reached, then β_0 decreases, i.e., $\beta_0 \to 0$, when $N_b \to \infty$ at $N_b > N_b^{max}$.

Important conclusion, following from our studies of the classical energy minima in the case of $O(6)$-limit Hamiltonian with cubic d-boson interaction, is that, in order to study triaxial nuclear shapes, one should take into account not just the $L' = 3$ term of cubic d-boson interaction operator, the role of which has been stressed in the literature until now (see [27, 16]), but the $L' = 4, 6$ terms as well, i.e., one should take into account the entire sum of cubic d-boson operator terms, as it has been pointed out also in [37]. Another significant conclusion is that triaxial equilibrium shape, obtained in the case of considered cubic d-boson interaction, is the effect due to finite boson number.

Another approach to the accounting of three-body interactions in the frameworks of IBM-1 has been proposed in [28]. They have considered the $O(6)$-limit Hamiltonian with attached cubic $O(6)$ quadrupole operator interaction term $[\mathbf{QQQ}]^{(0)}$. Such model allows to describe the $SU(3)$-type rigid rotator states based on the $O(6)$-symmetric γ-soft core, and to study, e.g., triaxial nuclei with observed β-vibrational band. In [28], two simple IBM-1 Hamiltonians have been proposed: 1) the H_1, conserving the dynamical $O(6)$-symmetry of the original $O(6)$-limit Hamiltonian, and 2) the H_2, which includes the $[\mathbf{QQQ}]^{(0)}$ term in the form, which is $O(6)$-symmetry non-conserving.

At the $N_b \to \infty$ limit, the classical energy functionals E_{ir} (see [28]) of both model Hamiltonians H_i $(i = 1, 2)$ can be presented via expression [R3]:

$$E_{ir}(\alpha\delta_{i,1} + \alpha'\delta_{i,2}, \vartheta; \beta, \gamma) = c_{i,1}\frac{\beta^2}{1+\beta^2} + c_{i,2}\frac{(1-\beta^2)^2\delta_{i,1} + \beta^2\delta_{i,2}}{(1+\beta^2)^2}$$
$$-4\vartheta\sqrt{\frac{8}{35}}\frac{\beta^3\cos(3\gamma)}{(1+\beta^2)^3}, \tag{19}$$

where $c_{i,1} = 4$ and $c_{i,2} = \alpha/4$, in the case of $i = 1$ model, and $c_{i,1} = 1$ and $c_{i,2} = 4\alpha'$, in the case of $i = 2$. Model parameters α and α' are related with those of the $O(6)$-limit of IBM-1; ϑ is a strength parameter of the cubic $[\mathbf{QQQ}]^{(0)}$ interaction. Since the classical energy expression Eq. (19) includes only the $\sim \cos(3\gamma)$ dependence, that means that the inclusion of $[\mathbf{QQQ}]^{(0)}$ terms allows one to obtain E_{ir} minima only at $\gamma_0 = 0°$ or $60°$ asymmetry angles: either prolate $(\beta_0 > 0, \vartheta > 0)$, or oblate $(\beta_0 < 0, \vartheta < 0)$. These solutions are completely symmetric with respect to ϑ sign.

The application of the minima condition gives one quartic equations for the quadrupole deformation parameter β. These equations have been analyzed, giving special attention to regions where there are only complex roots, corresponding to spherical nucleus.

Conditions for the prolate-oblate shape phase transition, related with the sign conversion of parameter ϑ, one can analyze looking for relationships $\beta_{0l}(\alpha, \vartheta) = -\beta_{0m}(\alpha, -\vartheta)$ in the case of both models. Position of the triple point where spherical and prolate-oblate deformed nuclear shapes coexist is determined by the condition (see, e.g., [34]):

$$\left.\frac{d^2 E_{ir}(\alpha\delta_{i,1} + \alpha'\delta_{i,2}, \vartheta; \beta, \gamma = 0)}{d\beta^2}\right|_{\beta=0} = 0. \tag{20}$$

The solution of obtained equation gives triple point coordinates at ($\alpha = 4, \vartheta = 0$), in the case of H_1 model ($i = 1$), and at ($\alpha' = -1/4, \vartheta = 0$), in the case of H_2 model ($i = 2$).

Comparison of our precise analytical solution results, obtained in the case of $O(6)$-symmetric model with cubic $[\mathbf{QQQ}]^{(0)}$ interaction, with those of Ref. [28] shows some discrepancies. So, in our approach, the spherical shape region forms a closed ellipsoid like figure. Opposite to it, in [28] the spherical shape region doesn't form a closed area. Phase transitions in the case of $O(6)$-symmetry non-conserving model with $[\mathbf{QQQ}]^{(0)}$ interaction were not considered in [28].

3 The study of quantum chaos in the case of geometrical rigid triaxial rotator models

Because of their Hamiltonian structure, geometrical nuclear models are rarely used for QPT studies at low energy and spin values. However, quantum chaos phenomena, related to spectroscopic characteristics of various geometrical models, especially at high angular momenta of nuclear core, have attracted notable attention during last decade. A considerable methodological interest for quantum chaos studies has the nuclear triaxial rotator model because its classical analogue is a well-known integrable system.

In our studies of quantum chaos criteria, we have considered two versions of the nuclear rigid triaxial rotator model: the Davydov's model, and Bravin-Fedorov's model. Most attention has been given to the calculation and comparison of dynamical quantum chaos criteria - the wave function entropy $W(\Psi_i)$, and the fragmentation width of basis states $\kappa(\Phi_k)$. The obtained results have been included in the journal paper manuscript [R4] and published in the proceedings of the international conference. The journal paper manuscript presently is revised and extended including data on quantum chaos statistical criteria calculations. Also, the results of our studies have been reported at the international [A5,A8] and local [A4,A6] scientific conferences in 2007 and 2008.

The Davidov's rigid triaxial rotator model (see, e.g., [29, 10]) is a simplest collective model which allows one to describe excited levels of even-even nucleus having a stable triaxial deformation with asymmetry angle $\gamma = \gamma_{eff} \neq 0$. In the case of rigid quadrupole deformation ($\beta = \beta_{eff}$, $\gamma = \gamma_{eff}$), one can present the collective nuclear core Hamiltonian as

$$H_D = \frac{1}{2} \sum_{j=1}^{3} \frac{\mathbf{I}_j^2}{\sin^2(\gamma - j\frac{2\pi}{3})}, \tag{21}$$

where $\mathbf{I}_j$ are the projections of the total nuclear angular momentum operator $\mathbf{I} \equiv \mathbf{L}$ on Descartian axes coinciding with principal directions of the nuclear momentum of inertia. Matrix elements of Hamiltonian Eq.(21) are evaluated in the basis formed by the axially-symmetric rotator eigenfunctions.

A more refined approach has been proposed by Bravin and Fedorov (see [30]). Their rigid triaxial rotator model Hamiltonian expression includes the dependence from both nuclear quadrupole deformation parameters β and γ.

Hamiltonian matrices of both triaxial rotator models have been diagonalized for all even and odd spin values in the range $I = 2, 3, \ldots, 100, 101$, i.e., up to maximal ranks $n_0(I_{even} = 100) = 51$, and $n_0(I_{odd} = 101) = 50$, giving energies of 2600 theoretical states: $E_1(I), E_2(I), \ldots, E_{n_0}(I)$. The diagonalization procedure has been performed at $N_\gamma = 28$ asymmetry angle values $\gamma = 3°, 4°, \ldots, 30°$. In the case of Bravin-Fedorov's model, calculations have been performed at three fixed β values: 0.1, 0.2, and 0.3. The obtained sets of eigenvalues and wave functions have been used for the study of statistical and dynamical quantum chaos criteria $P(S)$, $W(\Psi_i)$, and $\kappa(\Phi_k)$.

Statistical chaos criteria - the nearest level energy spacing distributions P(S) have been calculated in the case of maximal considered spin value $I = 100$, when the rank of diagonalized matrix is $n_0 = 51$. Although the number of eigenvalues in the unfolded spectrum at this spin value is small, if one compares it with those at $I \geq 1000$ values used in Ref. [38], one can see that our results allow to make similar conclusion: the level spacing distribution of the rigid triaxial rotator does not obey Poissonian statistics, as one could expect for the classically integrable Hamiltonian.

Table 2: Comparison of averaged wave function entropy $W(\Psi_i)_{av}(I)$ values with the theoretically possible maximal $W(\Psi_i)_{max}(I)$ values in the case of rigid triaxial rotator model.

I_{even}	I_{odd}	n_0	$W(\Psi_i)_{av}$		$W(\Psi_i)_{max}$	$W(\Psi_i)_{av}/W(\Psi_i)_{max}$	
			I_{even}	I_{odd}		I_{even}	I_{odd}
4	7	3	0.936	0.936	1.099	0.849	0.852
6	9	4	1.047	1.095	1.386	0.755	0.790
8	11	5	1.213	1.254	1.609	0.754	0.779
10	13	6	1.398	1.462	1.792	0.780	0.816
12	15	7	1.508	1.561	1.946	0.775	0.802
14	17	8	1.602	1.659	2.079	0.771	0.798
16	19	9	1.746	1.794	2.197	0.795	0.817
18	21	10	1.811	1.854	2.303	0.786	0.805
20	23	11	1.885	1.926	2.398	0.786	0.803
22	25	12	1.979	2.022	2.485	0.796	0.814
24	27	13	2.033	2.078	2.565	0.793	0.810
26	29	14	2.090	2.143	2.639	0.792	0.812
28	31	15	2.177	2.225	2.708	0.804	0.822

Fig. 3 shows the results of $P(S)$ calculations at different asymmetry angle γ values. The obtained distributions have been fitted by Brody formula Eq. (7), and the lower part of Fig. 3 presents the obtained value of Brody coefficient ζ in dependence on γ. One can see that the chaoticity of the system grows with asymmetry. For $18^\circ \leq \gamma \leq 29^\circ$, eigenvalues of the rigid triaxial rotator obey Wigner statistics characteristic to GOE. Note that, at $\gamma = 30^\circ$, the chaoticity of the system again is reduced. However, in order to make more confident conclusions, one should perform $P(S)$ distribution studies at higher spin values.

The entropy values $W(\Psi_i)_{av}(I)$, averaged over all wave function components at particular asymmetry angle γ, demonstrate a stable trend of $W(\Psi_i)_{av}(I)$ growth when γ is increased up to $\gamma = 30^\circ$. The maximal wave function entropy value is attained at $\gamma = 30^\circ$. This trend is observed both for even and for odd spin I values, and it is not affected by some value fluctuations in dependence from γ taking place in the case of separate $W(\Psi_i)$ components.

In Table 2, the averaged entropy values $W(\Psi_i)_{av}(I)$, calculated in the case

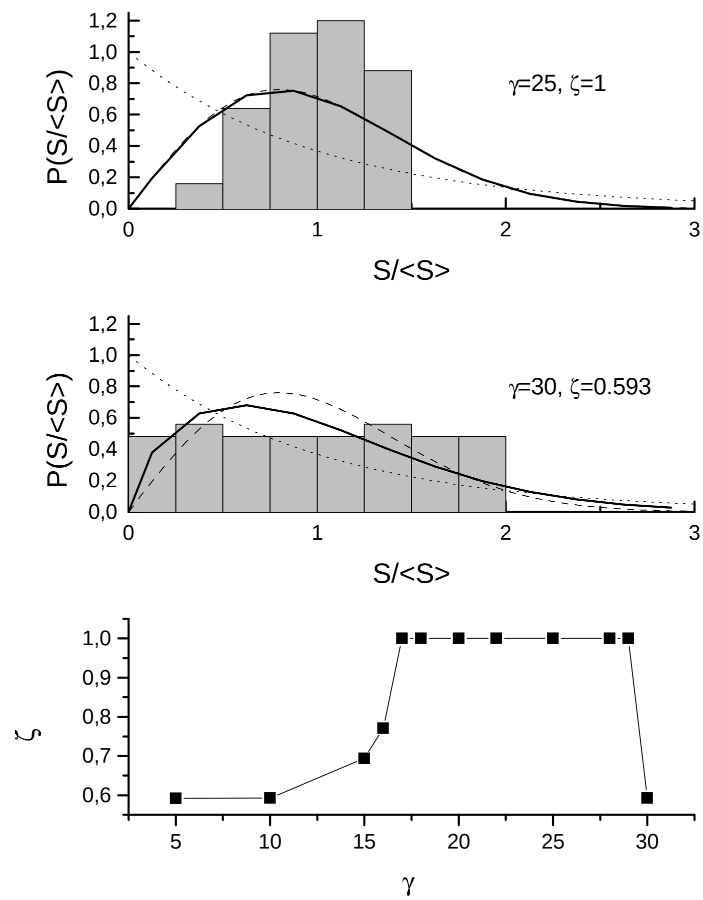

Figure 3: Nearest level spacing distributions P(S) in dependence from asymmetry angle γ in the case of rigid triaxial rotator model.

of maximally mixed basis state functions $\Phi_k(I, M, K)$ at $\gamma = 30°$, are compared with the theoretically possible maximal entropy values $W(\Psi_i)_{max}(I) = \ln(n_0(I))$, corresponding to the case when mixed perturbed wave functions are uniformly spread over all basis states. This comparison shows that, even in the case of maximal mixing, $W(\Psi_i)_{av}(I) = (0.75 \div 0.85) W(\Psi_i)_{max}(I)$. Therefore, the intrinsic structure of Davidov's rigid triaxial rotator model does not allow a higher degree of chaoticity with respect to axially-symmetric rotator eigenfunction basis.

Evaluation of another dynamical quantum chaos criterion - the fragmentation width of basis states $\kappa(\Phi_k)$ is a more complicated task. Calculation of Γ_{spr} values requires the control over the fulfillment of condition (10), imposed on mixing amplitudes of involved states. That means that $\kappa(\Phi_k)$ values can be evaluated only if the mixing of basis states exceeds certain limit, i.e. in the case of large asymmetry angle values. An example of $\kappa(\Phi_k)$ criterion calculation results at spin $I = 24$ one can find in Table 3. At this spin value, the rank $n_0(I = 24) = 13$, and one can start evaluating basis state fragmentation widths at $\gamma = 23°$. One can clearly recognize the trend of $\kappa(\Phi_k)_{av}$ value growth with increasing asymmetry angle γ.

It has been found that, in the case of rigid triaxial rotator models, one can study the theoretically predicted transition from the soft chaos to the hard chaos only starting with a comparatively high spin value ($I = 50$), when the number of basis states $n_0 \geq 26$. In our calculations, we have not observed a smooth gradual transition from the soft chaos ($\kappa(\Phi_k) < 1$) to hard chaos ($\kappa(\Phi_k) > 1$). In the rigid triaxial rotator model, transition to the hard chaos case is abrupt, and we can propose two explanations for such situation. The first one is related with the restriction (10), which considerably limits a number of states suitable for Γ_{spr} and $\kappa(\Phi_k)$ evaluation. The second one follows from the tridiagonal structure of the model Hamiltonian matrix. Due to this, the wave function mixing amplitudes are not smoothly spread over all basis function components: their distribution is approximately Lorentzian, which, in turn, increases the role of restriction Eq.(10) for the calculation of $\kappa(\Phi_k)$ values.

The results obtained for the values of both criteria: $W(\Psi_i)$ and $\kappa(\Phi_k)$, in the case of Bravin-Fedorov's model show the reducing of dynamical chaoticity if quadrupole deformation β is increased, which is as expected since we consider mixing with respect to axially-symmetric rotator basis functions.

In addition, we have performed the analysis of theoretical energy spectra, obtained in the case of both rigid triaxial rotator models, with the aim to

Table 3: Basis state fragmentation widths $\kappa(\Phi_k)$ of the rigid triaxial rotator model calculated at spin value $I = 24$ ($n_0(I) = 13$).

γ	$D_0(\gamma)$	$\kappa(\Phi_k)^a$									$\kappa(\Phi_k)_{av}$
		$k=3$	$k=4$	$k=5$	$k=6$	$k=7$	$k=8$	$k=9$	$k=10$	$k=11$	
23°	111.89	X	X	1.71	X	X	X	X	X	X	1.71
24°	98.21	X	X	X	2.15	X	X	X	X	X	2.15
25°	85.81	0.55	1.47	1.98	2.41	X	X	X	X	X	1.60
26°	74.46	1.39	1.69	3.82	X	3.18	X	X	X	X	2.52
27°	63.96	1.45	4.00	5.45	X	2.91	3.13	X	X	X	3.39
28°	54.14	1.48	5.98	7.45	3.97	3.50	3.02	3.15	X	X	4.08
29°	44.87	0.71	2.81	8.57	9.97	2.27	3.16	3.72	X	4.97	4.52
30°	36.00	7.33	3.50	3.50	10.00	6.50	5.33	4.67	5.50	4.50	5.65

[a] – States for which one cannot evaluate $\kappa(\Phi_k)$ value due to the violation of condition Eq.(10) are marked by "X".

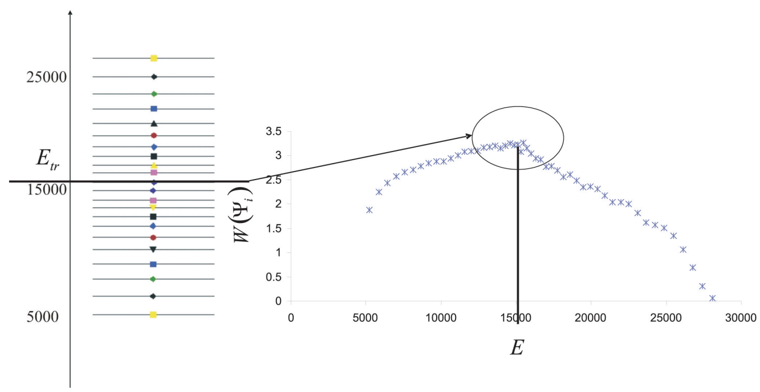

Figure 4: Transition from the rotational type spectrum to the librational type spectrum in the case of Davydov's rigid triaxial rotator model at $I = 100$ and $\gamma = 25°$.

search for the transition from the rotational type level sequence to the librational one. Such transition in the frameworks of semi-classical description [14] occurs at the energy value $E_{tr} = (b/2)I^2$, i.e., the quantum statistics of the rigid triaxial rotator model behaves analogously to that of another anomalous quantum system - the one-dimensional harmonic oscillator.

Characteristic maxima of energy level density $\rho(E_i)$, and corresponding wave function entropy $W(\Psi_i)$ have been observed at E_{tr} in dependence from I and γ, in the case of Davydov's model (see Fig. 4), and in dependence from I, β, and γ, in the case of Bravin-Fedorov's model. That agrees with the results of [14] obtained in the case of Davydov's rigid triaxial rotator model.

4 The study of QPT in the case of complete IBM-1 model

It was logical to continue our studies of nuclear shape phase transitions, which were started employing simplified versions of IBM-1, with the use of complete IBM-1 version. Standard IBM-1 Hamiltonian, depending on six degrees of freedom of one s-boson and five d-bosons, allows to describe complete dynamics of the even-even nuclear core collective excitations of the total model symmetry group $U(6)$ in terms of $U(5)$, $SU(3)$, and $O(6)$ subgroup chains Eq. (2). Complete IBM-1 Hamiltonian and its classical energy limit depend on six model parameters, therefore, in order to analyze their behaviour in the entire model parameter space, one requires special methods. In [8], the approach based in catastrophe theory has been proposed. Their method allows to reduce the analysis of IBM-1 classical energy functional to the study of its behaviour in the space of just two essential control parameters.

We have used the approach developed in [8] for our study of complete IBM-1 Hamiltonian classical energy E_{cl} surfaces employing the method of precise solution of minima condition equations developed in the case of simplified IBM-1 versions. The results of our studies have been published in a journal paper [R6] and reported at the international scientific conference in 2008 [A7].

Employing the catastrophe theory formalism (for details see [8]), the following essential control parameters are introduced:

$$r_1 = \frac{a_3 - u_0 + w}{2a_1 + w - a_3}; \qquad r_2 = -\frac{2a_2}{2a_1 + w - a_3}, \tag{22}$$

where $w = \varepsilon/(N_b - 1)$, and a_1, a_2, and a_3 are parameters that replace six initial two-boson interaction constants. Then, if one assumes $\gamma = 0°$, eliminating in such a way the γ-degree of freedom, one obtains following final expression for the classical energy functional of complete version of IBM-1:

$$E_0(r_1, r_2; \beta) = \frac{1}{(1+\beta^2)^2} \left[\beta^4 + r_1\beta^2(\beta^2 + 2) - r_2\beta^3\right]. \tag{23}$$

The classical energy functional $E_0(r_1, r_2; \beta)$ in the space of control parameters (r_1, r_2) has the form of a "swallow tail" diagram [8]. This diagram involves all limiting cases of IBM-1 dynamical symmetries ($U(5)$, $O(6)$, $SU(3)$, $\overline{SU(3)}$).

Let us consider a solution for the classical energy minimum problem. A corresponding equation one can obtain applying to Eq.(23) the extreme condition. If one excludes trivial solutions by imposing conditions $(1+\beta^2)^3 \neq 0$ and $\beta \neq 0$, one can reduce this extreme condition to a cubic equation

$$A\beta^3 + B\beta^2 + C\beta + D = 0. \tag{24}$$

The three roots β_{0i} $(i = 1, 2, 3)$ of this cubic equation give deformation parameter β values at which energy functional Eq.(23) has minima. The obtained explicit expressions for these roots are very cumbersome and, in general, complex functions of control parameters r_1 and r_2. The behaviour

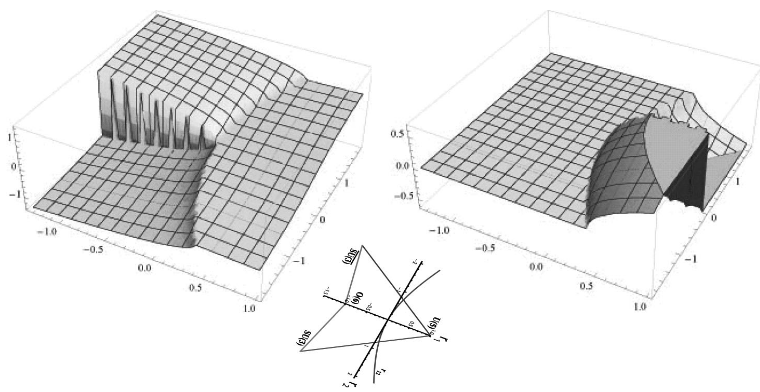

Figure 5: Behaviour of the real (left panel) and imaginary (right panel) parts of the first root β_{01} of Eq.(24) in the $-2 \leq r_1 \leq 2$, and $-2 \leq r_2 \leq 2$ range of control parameters.

of one of these roots within parameter value ranges $-2 \leq r_1 \leq 2$, and $-2 \leq r_2 \leq 2$ is shown in Fig. 5 separately for real and imaginary parts.

Main features of these roots one can analyze, analogously as it has been done in the case of simplified IBM-1 versions, by considering values of the cubic equation (24) discriminant D_3. When $D_3 < 0$, one has one real, and two complex conjugated roots. If $D_3 > 0$, there are three real, unequal roots, while at $D_3 = 0$ - two real, equal roots.

The $D_3 = 0$ case with two real degenerate roots defines the second order phase transition line between spherical and deformed nuclear shapes:

$$\begin{pmatrix} r_{11} \\ r_{12} \end{pmatrix} = \mp \frac{(9r_2^2 + 16)^{3/2}}{54 r_2^2} - \frac{32}{27 r_2^2} - 1. \tag{25}$$

These solutions coincide with those given by Eqs.(3.19 a,b) of Ref. [8] where the lines r_{11} and r_{12} define, according to the catastrophe theory, the bifurcation set as the locus of points in the space of control parameters (r_1, r_2) at which a transition occurs from the one local minimum to another. In our case, the r_{12} solution defines the arc line, separating spherical and deformed shape areas, while the r_{11} solution has no such clear physical interpretation.

The triple point, where spherical and both deformed (prolate and oblate) shapes meet, one can obtain from the critical point condition imposed on the second-order derivative of Eq.(23):

$$\left.\frac{d^2E_0(r_1,r_2;\beta)}{d\beta^2}\right|_{\beta=0} = 0, \tag{26}$$

which gives one the coordinates of this point at $r_1 = r_2 = 0$.

In the bottom "deformed shape" part below the r_{12} arc line defined by Eq.(25), we have the $D_3 > 0$ case with three real and unequal roots. The numerical values for two of them: (β_{01}, and β_{03}), are mirror symmetric and have opposite signs with respect to the $r_2 = 0$ line. The second root β_{02} has a close to zero value far from the $r_2 = 0$ line in the entire (r_1, r_2) area on both sides of the r_{12} arc line, and nonphysically large values $\beta_{02} \to \pm\infty$ with opposite signs along the entire length of the $r_2 = 0$ line when $r_2 \to \pm 0$.

In the top "spherical shape" part of the diagram we have the $D_3 < 0$ case with two complex conjugated roots β_{01}, β_{03}, which are mirror-symmetric with respect to $r_2 = 0$ line. These roots have very small real parts and large imaginary parts with opposite signs. The behaviour of the second real root β_{02} in this area is similar to that decribed above in the $D_3 > 0$ case.

In order to compare the results of our precise solution method for the classical energy functional minima problem with the results obtained using the Landau theory approach we have expanded Eq.(23) in Taylor series with respect to deformation parameter β.

$$E_{0T}(r_1,r_2;\beta) = 2r_1\beta^2 - r_2\beta^3 + (1-3r_1)\beta^4 + 2r_2\beta^5 + (4r_1-2)\beta^6 + O(\beta^7). \tag{27}$$

If one applies extreme condition to this expression, one obtains equation for the classical energy minimum.

In the frameworks of approach based on the Landau theory of phase transitions, higher order terms in Eq.(27), starting with the $\sim \beta^4$ power term, are usually disregarded (see, e.g., [20]). In order to assess the effects due to cut-off of this expansion, we have applied extreme condition to corresponding Taylor series including subsequently all terms up to β^4, up to β^5, and up to β^6. It has been found that only the inclusion of power terms up to β^5 allows one to obtain a cubic equation (with the condition $\beta \neq 0$), in which only two coefficients, those at β^3 and β^2, slightly differ from corresponding coefficients in the equation Eq. (24) obtained via a precise solution method. Analysis of the three roots of this cubic equation gives a similar picture of phase transition critical points and lines as in the case of precise solution. However, if one cuts off the Taylor expansion (27) at β^4 or β^6 power terms, one obtains nonphysical values of corresponding roots β_{0i}.

5 The study of prolate-oblate shape phase transition in the case of $A \sim$190 region nuclei

Analysis of experimental data shows that the nuclear shape phase transition in the W-Os-Pt region has a very complex nature. In fact, two parallel transitions take place: the $SU(3) - O(6) - \overline{SU(3)}$ phase transition from the deformed prolate shape to the oblate one, and the deformed-to-spherical $O(6) - E(5) - U(5)$ transition due to the nearness of the $N = 126$ shell closure. Therefore, one must consider the variation of IBM-1 parameters in the entire model parameter space, not just along some selected phase transition critical line. So, in order to obtain a realistic theoretical description for specific nuclei, we have employed the complete IBM-1 Hamiltonian presented in multipole form Eq.(3).

Model calculations for each nucleus have been performed at boson number N_b determined by the sum of proton hole pairs with regards to closed $Z = 82$ shell, and neutron hole pairs with regards to closed $N = 126$ shell. The computer code PHINT [17] was used for the diagonalization of the model Hamiltonian in order to obtain corresponding eigenvalues and eigenfunctions in the spherical $U(5)$ basis. The parameters of IBM-1 Hamiltonian: $\varepsilon', \eta, \chi, \kappa$, and ω, have been varied in order to achieve a best possible agreement with available experimental data [32] in the case of each selected nucleus. These data included the energies of confidently established low-lying levels with spin values $I \leq 8$ (in the case of ground state band), and with $I \leq 6$ (in the case of other collective excitations). In such a way, the entire known low-lying collective part of the excited level scheme has been involved for the study of nuclear shape phase transition. Usually, only a ground state or a few lowest levels are taken into account (see, e.g., [33]).

In order to facilitate the fit of IBM-1 model parameters, their starting values were obtained via the least squares method solution of linear equation systems for experimental and theoretical level energy values either in the $SU(3)$-limit of axially-symmetric rotator, or in the $O(6)$-limit of γ-unstable nucleus. The hexadecapole deformation term of Eq. (3) has been disregarded assuming $\xi = 0$.

Since the IBM-1 Hamiltonian is symmetric with respect to the sign of the prolate-oblate phase transition control parameter χ, we have performed our level energy calculations at $\chi \leq 0$ values, assigning the sign of χ later with regards to the experimentally observed electromagnetic properties, and taking into account the behaviour of model parameters in neighbouring nuclei.

The obtained values of IBM-1 parameters for all considered tungsten, osmium, and platinum isotopes are summarized in Table 4. Agreement between experimental and calculated level energies is characterized by the mean square deviation $d = \sqrt{(E_{exp} - E_{calc})^2/m}$, where m is the number of experimental levels included in the fit. One can see that the agreement which can be achieved in the frameworks of IBM-1 improves for nuclei towards the $SU(3)$-limit. In the case of $O(6)$-limit nuclei, the overall quality of the fit for all involved experimental levels is notably worse, and the dependence on χ value is more pronounced. The prolate-oblate phase transition is abrupt, especially for osmium and tungsten nuclei.

It has been found that the employed IBM-1 version does not allow to describe with good quality all observed low-energy levels of considered nuclei in the vicinity of phase transition critical line $E(5) - O(6)$. If one can successfully reproduce the $K^\pi = 0^+$ ground state band, and the $K^\pi = 2^+$ quasi γ-band levels, then, if one includes observed additional collective 0^+ and 4^+ states, they would not fit together. Again, the model parameter values, which improve the description of these additional states, would shift the odd spin levels of the quasi γ-band too far away from their experimental values. Such behaviour can be explained by the complex nature of observed phase transition taking place at different critical parameter χ values in dependence from excitation energy, i.e., one observes a coexistence of prolate and oblate shapes in the same nucleus (see, e.g., [39]).

Farther away from the $O(6)$ critical point, one can successfully describe all experimental levels up to 2.5 MeV with the same IBM-1 parameter set. Moreover, parameter sets for neighbouring nuclei towards the $SU(3)$-limit are similar, which is not the case in the vicinity of the $O(6)$-limit. It means that one should be most careful when adopting for IBM model calculations parameter values used earlier for neighboring nuclei - such approach is not applicable for nuclei belonging to transitional deformation regions.

In the last two columns of Table 4, the values of control parameters r_1 and r_2, employed in the catastrophe theory analysis of nuclear shape phase transitions are given. The use of these parameters allows one to associate the complete IBM-1 model parameter set $(\varepsilon', \eta, \kappa, \omega, \xi, \chi)$, obtained for each of considered nuclei, with the point within the "swallow-tail" phase diagram, characterizing nuclear deformation and its stability. The values of control parameters obtained for $184 \leq A \leq 194$ isotopes of W, Os, and Pt are

Table 4: IBM-1 parameter values of $184 \leq A \leq 194$ region W, Os, and Pt nuclei

Nucleus	N_b	ε' (MeV)	κ (MeV)	η (MeV)	ω (MeV)	χ	m	d (MeV)	r_1	r_2
^{184}W	12	0.024	-0.03094	0.0263	-0.00420	-1.17170	12	0.0155	-0.87412	1.31552
^{186}W	11	0.017	-0.03096	0.0290	-0.00412	-1.13056	12	0.0451	-0.82056	1.22351
^{188}W	10	0.008	-0.04480	0.0112	0.01080	-0.19230	9	0.0455	-0.57963	0.16004
^{184}Os	12	0.028	-0.03300	0.0272	-0.00340	-1.11133	12	0.0253	-0.82736	1.20022
^{186}Os	11	0.025	-0.04400	0.0276	-0.00420	-0.67082	12	0.0280	-0.74747	0.65199
^{188}Os	10	0.026	-0.07900	0.0170	-0.00700	-0.31305	11	0.0775	-0.79163	0.30385
^{190}Os	9	0.010	-0.07500	0.0142	0.00100	-0.10733	13	0.0907	-0.70298	0.09769
^{192}Os	8	0.005	-0.06650	0.0185	0.00160	-0.11180	13	0.1069	-0.63925	0.09788
^{194}Os	7	0.005	-0.09500	0.0150	-0.00200	0.12969	7	0.0657	-0.67312	-0.11630
^{184}Pt	12	0.015	-0.02440	0.0175	0.01360	-0.55902	12	0.0970	-0.43119	0.42030
^{186}Pt	11	0.015	-0.02450	0.0195	0.01100	-0.55902	12	0.0631	-0.42336	0.42120
^{188}Pt	10	0.012	-0.04000	0.0255	0.00900	-0.15652	11	0.0977	-0.50327	0.12400
^{190}Pt	9	0.009	-0.08100	0.0190	0.00235	-0.06261	13	0.0891	-0.68075	0.05615
^{192}Pt	8	0.013	-0.08400	0.0195	0.00300	0.00894	12	0.1471	-0.63467	-0.00780
^{194}Pt	7	0.005	-0.09200	0.0195	0.00210	0.08050	13	0.1445	-0.61535	-0.06942

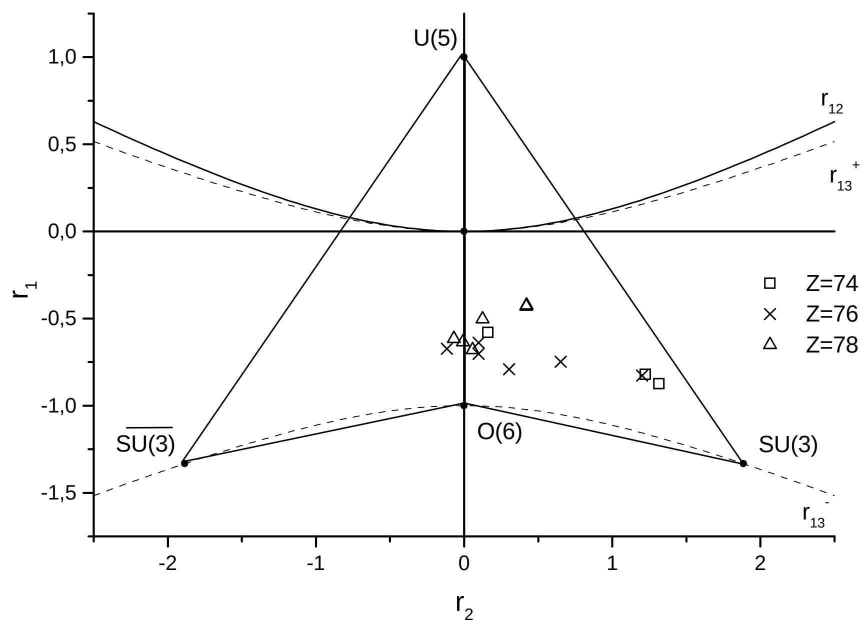

Figure 6: The values of catastrophe theory control parameters r_1, r_2 obtained for W, Os, and Pt nuclei with $184 \leq A \leq 194$.

displayed as points in the (r_1, r_2) parameter space diagram (Fig. 6). One can see that all considered nuclei belong to the domain below the r_{12} bifurcation set Eq. (25) separating spherical and deformed nuclei.

Now, let us consider the Maxwell sets of points in the (r_1, r_2) parameter space. At these points, classical energy surface assumes same value for two or more different critical values of control parameter, i.e., a coexistence of different shapes becomes possible. Maxwell sets, associated with the energy surface minimum (r_{13}^+), and maximum (r_{13}^-) at β_c=0, are defined by equation [8]:

$$r_{13}^{\pm} = -\frac{1}{2} \pm \frac{1}{2}\sqrt{1 + \frac{r_2^2}{2}}. \tag{28}$$

Another Maxwell set - for $\beta_c = \sqrt{r_1}$, forms a locus of points on the negative r_1 semi-axis at r_2=0; this set of points coincides with the $E(5)-O(6)$ critical line between prolate $r_2 > 0$, and oblate $r_2 < 0$ deformed shapes.

The performed study of the complete IBM-1 version classical energy functional shows that it has a well defined prolate minimum ($\beta > 0$) in the region $r_{13}^{-} < r_1 < 0$, in which the values of control parameters for all considered $184 \leq A \leq 194$ nuclei are located. An additional oblate minimum is a saddle point, unstable with respect to nuclear asymmetry parameter γ. It means that at higher excitations both prolate and oblate structures are allowed, and a possibility of such coexistence grows when r_1 value approaches zero. When $\beta < 0$, the picture is mirror symmetric with respect to r_1 negative semi-axis: one has a stable oblate minimum with a γ-unstable prolate saddle point.

As one can expect, the ^{184,186}W nuclei are close to the stable axially-deformed $SU(3)$-limit. Those of considered nuclei which have $|r_2| \leq 0.2$ (see Table 4) are situated in the region where nuclear shape changes from prolate to oblate. In in [6], it has been shown that χ is the control parameter of a prolate-oblate phase transition with critical point at $\chi = 0$ corresponding to $O(6)$-limit. In reality, this phase transition can occur at any point on the line connecting the $E(5)$ triple point of the Casten's triangle with the $O(6)$-symmetry point in the middle of the line connecting maximal quadrupole deformation points $SU(3)$ and $\overline{SU(3)}$. We have assigned plus sign to χ values of ^{192,194}Pt nuclei with regard to their experimental electric quadrupole moment Q values. The plus sign for χ value of ^{194}Os, for which there are no Q measurement data, is predicted from the observed dependence of r_2 values in neighbouring osmium nuclei. The obtained location of (r_1, r_2) points for ^{184,186}Pt indicate that these nuclei have prolate ground state band and oblate excited bands. With high probability, similar shape coexistence is present also in the case of ^{188}W.

In order to study relationships between nuclear shape phase transition and quantum chaos in the $A \sim$190 region, we have performed the analysis of statistical and dynamical quantum chaos criteria in dependence from the $SU(3) - O(6) - \overline{SU(3)}$ phase transition control parameter χ, as well as in terms of catastrophe theory essential control parameters r_1, r_2.

At first, let us consider the statistical criteria of quantum chaos - the nearest level spacing distribution $P(S)$. For this purpose, we have taken all obtained IBM-1 eigenvalues with spins ranging from 0 to 8 and created the unfolded theoretical energy spectrum for each nucleus. The results of the fit of Brody parameter ζ in the case of all 15 considered nuclei are presented in Table 5. Quality of the least-squares fit is characterized by $d' = \sum_{i=1}^{m'}(P(S/<S>) - P_B(S/<S>))^2$, where m' is the number of level

Table 5: Results of the fit of nearest level spacing distributions $P(S)$ for $184 \leq A \leq 194$ W, Os, and Pt nuclei.

Nucleus	N_b	m'	$< S >$	σ_S^2	ζ	d'
^{184}W	12	205	0.0252	0.0017	0.000	0.041
^{186}W	11	169	0.0267	0.0020	0.000	0.050
^{188}W	10	137	0.0476	0.0183	0.000	0.623
^{184}Os	12	205	0.0265	0.0020	0.000	0.041
^{186}Os	11	169	0.0306	0.0023	0.000	0.052
^{188}Os	10	137	0.0453	0.0028	0.000	0.052
^{190}Os	9	108	0.0452	0.0024	0.056	0.046
^{192}Os	8	83	0.0474	0.0022	0.081	0.024
^{194}Os	7	61	0.0636	0.0034	0.606	0.028
^{184}Pt	12	205	0.0427	0.0096	0.000	0.169
^{186}Pt	11	169	0.0396	0.0042	0.120	0.010
^{188}Pt	10	137	0.0454	0.0029	0.000	0.033
^{190}Pt	9	108	0.0525	0.0029	0.169	0.011
^{192}Pt	8	83	0.0604	0.0036	0.307	0.025
^{194}Pt	7	61	0.0696	0.0044	0.112	0.025

spacings. Additional characteristics of the $P(S)$ distribution are the mean value of S and its variance σ_S^2. Increased mixing is indicated by the growth of mean level spacings when one moves away from the $SU(3)$-limit.

One can see that the form of $P(S)$ distribution changes very slowly from the $SU(3)$-limit side: in the case of W and Os nuclei with $A \leq 188$, one cannot practically distinguish $P(S)$ from the Poisson form. On the contrary, in the vicinity of the $E(5) - O(6)$ critical line, a drastic change of chaoticity between neighboring isotopes is observed reflecting instability of nuclear shape and complex nature of observed phase transition.

Statistical quantum chaos criterion $P(S)$ characterizes distribution of Hamiltonian eigenvalues and, therefore, it is independent from model diagonalization basis. Behaviour of system's dynamical quantum chaos criteria characterizes its deviation from the symmetry properties inherent to the Hamiltonian of the chosen regular system. Wave function entropy $W(\Psi_i)$, just like fragmentation width of basis states $\kappa(\Phi_k)$, or any other dynamical quantum chaos criterion, evaluated using wave functions of considered states, depends on the choice of Hamiltonian diagonalization basis. Complete IBM-1 Hamiltonian is usually diagonalized in the $U(5)$-symmetric basis of the five-dimensional spherical harmonic oscillator eigenfunctions, while the prolate-to-oblate shape phase transition is mostly analyzed in the $SU(3)$-symmetric axial-rotator wave function basis (see, e.g., [6]). However, we have already noted that, for nuclei belonging to the $A \sim$190 region, the $O(6)$ critical point should be considered rather as the $E(5) - O(6)$ critical line with a considerable influence from the deformed-to-spherical transition. Therefore, we believe that it is justified to perform IBM-1 Hamiltonian diagonalization in the spherical $U(5)$-limit basis, and to consider critical behaviour of dynamical quantum chaos criteria from that point of view.

Fig. 7 presents the evaluated $W^{U(5)}(\Psi_i)$ values in dependence from the $SU(3) - O(6) - \overline{SU(3)}$ phase transition control parameter χ. One can see that $W^{U(5)}(\Psi_i)$ attains its maximal value in the $SU(3)$-limit and gradually decreases towards the $O(6)$ critical point. The slope of this dependence increases with the boson number N_b, which corresponds to experimentally observed picture that phase transition in the case of tungsten isotopes is more abrupt than in the case of platinum [39].

The analysis of obtained data allows to make following conclusions:

a) maximal dynamical quantum chaos criteria values, for all $184 \leq A \leq 194$ tungsten, osmium, and platinum nuclei, except ^{192}Pt, are obtained for states with spin values $I = 2$. That differs from the case of statistical chaos, when maximal chaoticity in all cases was observed for $I = 0$ states. Though, if one considers dynamical chaos relative to corresponding $W_{max}(n)$ value, then one obtains maximal ratio in the case of $I^+ = 0_1^+$ ground state for nuclei in the vicinity of critical line $E(5) - O(6)$;

b) the values of dynamical chaos criteria decrease towards $E(5) - O(6)$ critical line, along with the value of prolate-oblate phase transition control parameter χ, and towards the r_{12} bifurcation set, along with the value of control parameter $|r_1|$ (see Table 4). Such behaviour is characteristic to IBM-1 wave functions evaluated in the spherical $U(5)$ basis;

c) in the case of nuclei with $SU(3)$-type spectrum, maximal wave function entropy values are obtained for $I = 2_2$ states, i.e., the $K^\pi = 2^+$ γ-vibration band-heads, while in the case of nuclei with $O(6)$-type spectrum, maximal wave function entropy values are inherent to levels of the $K^\pi = 0^+$ ground state band;

d) in each isotope chain, the least dynamical chaos criterion values are obtained for nuclei which are closest to the prolate-oblate shape phase tran-

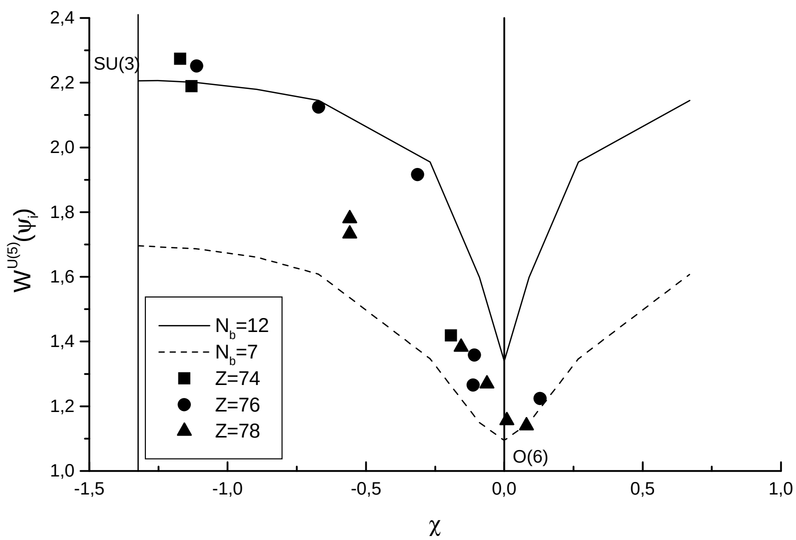

Figure 7: Values of the $I = 0^+$ ground state wave function entropy $W^{U(5)}(\Psi_i)$ in dependence from phase transition control parameter χ for $184 \leq A \leq 194$ W, Os, and Pt nuclei. Solid line shows the theoretical χ-dependence for $N_b = 12$ (at ^{184}W $SU(3)$-limit parameters), while dashed line – for $N_b = 7$ (at ^{194}Pt $O(6)$-limit parameters).

sition critical line $E(5) - O(6)$: the ^{188}W, ^{190}Os, and ^{192}Pt, correspondingly.

The behaviour of quantum chaos criteria, calculated using algebraic complete IBM-1 version, one can compare with that observed in the frameworks of geometric rigid triaxial rotator models.

Wave function entropy in the case of rigid triaxial rotator model rapidly increases towards $\gamma = 30°$. Dependence from the quadrupole deformation parameter β is weaker, displaying the decrease of wave function entropy for greater β values. On the contrary, the minima of the classical energy of IBM-1 Hamiltonian do not depend on the nuclear asymmetry angle γ value, i.e., the obtained energy saddle-points are γ-unstable [8]. However, it is generally assumed that $\gamma = 0°$ in the $SU(3)$-limit of prolate deformation, $\gamma = 30°$ in the γ-unstable $O(6)$-limit, and $\gamma = 60°$ in the case of oblate $\overline{SU(3)}$-symmetric rotator. The $O(6)$-limit is the critical point both for β- and γ-deformations [6]. Experimental data do not provide distinction between static and dynamic nuclear triaxiality. Therefore, such comparison between IBM-1 and rigid triaxial rotator results can take place.

However, in order to perform quantitative comparison of dynamical quantum chaos criteria evaluated in the frameworks of both model approaches, one should use IBM-1 wave functions obtained via the diagonalization of model Hamiltonian in the axially-symmetric $SU(3)$-limit wave function basis, employed also for the diagonalization of geometrical rigid triaxial rotator model Hamiltonians. Such detailed comparison is a theme for future studies.

6 Conclusions

Let us characterize fulfillment of the aims set for this dissertation work (see Sect. 1.2) by summarizing the results obtained in our studies of nuclear shape phase transitions and quantum chaos in the frameworks of geometrical and algebraic models of even-even nuclei.

1. Precise analytical expressions for the classical energy functional E_{cl} minima conditions in terms of nuclear quadrupole deformation parameter β have been obtained in the case of several algebraic interacting boson model versions:

a) the simplified two-parameter Casten's version of IBM-1;

b) the $O(6)$-limit Hamiltonian with included cubic d-boson interaction;

c) the $O(6)$-limit Hamiltonian with included cubic quadrupole operator term $[\mathbf{QQQ}]^{(0)}$ in two variants - the $O(6)$-symmetry conserving, and the

$O(6)$-symmetry non-conserving;

d) the complete IBM-1 version.

Corresponding classical energy surfaces have been analyzed in terms of spherical-to-deformed, and prolate-to-oblate nuclear shape phase transitions in dependence on IBM-1 model parameter values. It has been found that:

a) the results of our approach to the minimum problem of the classical energy functional in the case of simplified Casten's version of IBM-1 allow one to obtain precise values of deformation parameter β at each (η, χ) point of Casten's triangle. The obtained roots β_{0i} $(i = 1, 2, 3)$ of the cubic equation for E_{cl} minima condition are complicated and, in general, complex functions from the total boson number N_b and IBM-1 model parameters. These expressions are well suited for the analysis of phase transition lines and critical points, as well as for other studies involving the considered model;

b) in the case of $O(6)$-limit IBM-1 Hamiltonian with cubic d-boson interaction term, one can obtain the minimum of E_{cl} expression corresponding to stable triaxial deformation only if one takes into account the sum of all three-boson interaction terms with moments $L' = 0, 2, 3, 4, 6$, and not just the $L' = 3$ term, as it has been supposed earlier. Also, it has been shown that this triaxial shape minimum is an effect due to finite number of bosons, disappearing at $N_b \to \infty$;

c) in the case of $O(6)$-limit Hamiltonians with attached cubic $[\mathbf{QQQ}]^{(0)}$ term, main attention has been given to the study of regions where E_{cl} expression minima condition equations have only complex roots. The boundaries of these regions define phase transition from spherical shape to deformed ones. Also, conditions for the prolate-oblate phase transition, as well as for the triple point of deformations have been analyzed. Analysis has been performed for both versions of the model Hamiltonian - the $O(6)$-symmetric, and the $O(6)$-non-symmetric.

In the case of $O(6)$-symmetric model version, our results, obtained employing precise solution method, have shown that the spherical shape region forms a closed ellipsoid like figure, contrary to the earlier results obtained in Ref. [28]. The analysis of shape phase transition conditions in the case of $O(6)$-non-symmetric Hamiltonian version was not given previously by other authors;

d) the detailed analysis of minima conditions for the classical energy functional $E_{cl}(r_1, r_2; \beta)$ of complete IBM-1, performed using obtained precise expressions for three roots β_{0i} $(i = 1, 2, 3)$ of the cubic equation, similar to that in the case of simplified Casten's version, allowed to determine coordinates for phase transition critical lines and points in the space of catastrophe theory essential control parameters r_1 and r_2. Properties of the real and imaginary parts of roots β_{0i} have been analyzed in the "spherical" and "deformed" parts of the control space diagram;

e) the classical energy E_{cl} minima conditions obtained using the precise solution method have been compared with the ones obtained employing the approach of the Landau theory of phase transitions, in which the higher order terms of E_{cl} expansion are disregarded. In the case of simplified Casten's version of IBM-1, the qualitative conclusions drawn in our analysis of phase transition critical lines and points are similar to those obtained employing the Landau theory approach. However, analytical solution of the classical energy minimum problem allows to obtain more precise numerical values of β_0, and $E_{cl}(N_b, \eta, \chi; \beta_0)$.

In the case of complete IBM-1 version, the effects due to accounting of higher order terms of E_{cl} expansion have been assessed. It has been found that, in order to obtain the classical energy minima condition similar to that obtained via a precise solution method, one should take into account in such E_{cl} expansion all power terms up to β^5. The usual practice to consider just $\sim \beta^2$ and $\sim \beta^3$ terms can give distorted results. Therefore, if one can obtain precise analytical solutions of equations for the classical energy functional minimum conditions, then such approach to the study of nuclear shape phase transitions is preferable to the use of approximate Landau theory method.

2. Statistical - the nearest level energy spacing distribution $P(S)$, and dynamical - the wave function entropy $W(\Psi_i)$ and fragmentation width of basis states $\kappa(\Phi_k)$, quantum chaos criteria have been evaluated in the frameworks of algebraic simplified Casten's version of IBM-1, and in the case of two geometric rigid triaxial rotator models of even-even nuclei - Davydov's model, depending on asymmetry angle γ only, and Bravin-Fedorov's model, depending on both quadrupole deformation parameters γ and β. Behaviour of quantum chaos criteria has been analyzed both in terms of nuclear quadrupole deformation parameters and in terms of shape phase transition control parameters in the space of Casten's triangle. Dependence from nuclear spin and rank of diagonalized model Hamiltonian matrix has been studied as well.

In the case of simplified Casten's version of IBM-1, values of statistical and dynamical quantum chaos criteria have been calculated at $N_b = 8$ in selected points within the (η, χ) parameter space represented by Casten's triangle. Values of model parameters have been chosen in the range from below the $X(5) - E(5) - \overline{X(5)}$ phase transition line separating spherical and deformed shapes to the $SU(3)-O(6)-\overline{SU(3)}$ line corresponding to maximal deformation.

The results of quantum chaos statistical criterion calculations show that the simplified Casten's version of IBM-1 at $N_b = 8$ is quite regular. The deviation of nearest level spacings distributions $P(S)$ from the Poisson form is very slight even in the case of maximal mixing farther away from the vertexes of Casten's triangle. At such relatively low boson numbers, $P(S)$ distribution is strongly influenced by the model basis cut-off which affects the energies of higher spin states.

The results of dynamical quantum chaos criteria calculations show that, on the $U(5)-SU(3)$ line and in the area near it (with $\chi = 0.75 \cdot \chi_{max}$), the behaviour of $\kappa(\Phi_k)_{av}$ and $W(\Psi_i)_{av}$ values is correlated: increasing from the middle part (with $0.75 \cdot \eta_{E(5)} = 0.5625$) to the bottom line ($\eta = 0$). The correlation between $\kappa(\Phi_k)_{av}$ and $W(\Psi_i)_{av}$ values with respect to parameter χ value, when it changes in the direction from the $X(5)-SU(3)$ line towards the first order phase transition line $E(5)-O(6)$, is lost when mixing increases.

The results of quantum chaos calculations in the case of Davydov's model, and in the case of Bravin-Fedorov's model, performed at three different β values, have shown that the behaviour of quantum chaos criteria in the case of rigid triaxial rotator depends mostly on the triaxiality angle γ, the dependence on β is negligible. Maximal values of dynamical quantum chaos criteria are attained at $\gamma = 30°$ both for even and odd spin I values. Statistical chaoticity of the rigid triaxal rotator is maximal ($\zeta = 1$) at $18° \leq \gamma \leq 29°$; system's regularity increases again at $\gamma = 30°$.

In the case of geometrical rigid triaxial rotator models, it has been shown that the averaged wave function entropy values $W(\Psi_i)_{av}$, even for maximal mixing of basis states (at $\gamma = 30°$), reach only about 75-85 % of the theoretically possible maximal $W(\Psi_i)_{max}$ values. That indicates that the intrinsic structure of the rigid triaxial rotator model does not allow a higher degree of chaoticity with respect to axially-symmetric rotator eigenfunction basis. Because one has to control fulfillment of the condition (10), imposed on mixing amplitudes of involved states, one can evaluate another dynamical quantum chaos criterion $\kappa(\Phi_k)$ only if the mixing of basis states exceeds certain limit, i.e., in the case of large asymmetry angle values.

The results of quantum chaos dynamical criteria calculations in the case of Bravin-Fedorov's model show that the values of both criteria: $W(\Psi_i)$ and $\kappa(\Phi_k)$, become smaller when the value of quadrupole deformation parameter β is increased, which is as expected since the unperturbed system is an axially-symmetric rotator.

Analysis of the obtained theoretical energy spectra of rigid triaxial rotator models allowed to observe characteristic maxima of energy level density and wave function entropy at $E_{tr} \approx (b/2)I^2$, corresponding to transition from the rotational type level sequence to the librational one. Such transition demonstrates [14] that quantum statistics of the rigid triaxial rotator model behaves analogously to that of another anomalous quantum system - the one-dimensional harmonic oscillator. This transition has been studied in dependence from I and γ in the case of Davydov's model, and in dependence from I, β, and γ in the case of Bravin-Fedorov's model.

3. A possibility to use the basis state fragmentation width $\kappa(\Phi_k)$ as the dynamical quantum chaos criterion has been studied in the case of algebraic Casten's version of IBM-1, and in the case of geometrical rigid triaxial rotator models. It has been shown that $\kappa(\Phi_k)$ can be successfully applied for characterization of quantum chaos inherent to model Hamiltonian with respect to chosen eigenfunction basis of unperturbed quantum system, just like the generally used wave function entropy $W(\Psi_i)$. Correlation between both criteria has been observed in the inner regions of Casten's triangle below the $X(5)-E(5)-\overline{X(5)}$ second order phase transition line between spherical and deformed shapes in the direction of the $SU(3)-O(6)-\overline{SU(3)}$ basis line.

The use of basis state fragmentation width criterion allows one to apply additional grouping of model Hamiltonian states according to their $\kappa(\Phi_k)$ value: separating soft quantum chaos states with $\kappa(\Phi_k) < 1$, and hard quantum chaos states with $\kappa(\Phi_k) > 1$. Averaged $\kappa(\Phi_k)_{av}$ values then characterize the dynamical chaoticity of the perturbed system as a whole. It has been found that the theoretically predicted transition from the soft chaos to the hard chaos, in the case of rigid triaxial rotator models, can be studied only starting with a comparatively high spin value ($I = 50$), when the number of basis states $n \geq 26$.

In our calculations, we have not observed a smooth gradual transition from the soft chaos ($\kappa(\Phi_k) < 1$) to hard chaos ($\kappa(\Phi_k) > 1$), i.e., in the rigid triaxial rotator model, transition to the hard chaos case is abrupt, which can be explained by the tridiagonal structure of the model Hamiltonian matrix, which increases the role of restriction Eq.(10) for the calculation of $\kappa(\Phi_k)$ values.

4. The developed theoretical methods of quantum phase transition and quantum chaos studies have been applied for the analysis of prolate-oblate shape phase transition in the tungsten, osmium, and platinum isotope chains

belonging to the transitional $A \sim 190$ region. Nuclei of these three elements have shapes ranging from the stable prolate axial-symmetry to the asymmetric γ-unstable form.

The energies and wave functions of low-lying collective states in the case of 15 even-even nuclei with $184 \leq A \leq 194$ have been calculated employing complete version of IBM-1. Model parameter values for each nucleus have been determined via the fit to all experimentally observed level energies with $I \leq 8$, in the case of ground state band, and $I \leq 6$, in the case of other collective excitations. Relationships between shape phase transitions and quantum chaos criteria: $P(S)$, and $\overline{W(\Psi_i)}$, have been analyzed: a) in dependence on the $SU(3) - O(6) - \overline{SU(3)}$ prolate-oblate shape phase transition control parameter χ; b) in dependence on catastrophe theory control parameters r_1 and r_2; c) in dependence on proton and neutron numbers Z and N; d) in dependence on level spin I.

A good agreement has been obtained in the case of nuclei with stable prolate deformation, while, in the phase transition region close to the $E(5) - O(6)$ critical line, one cannot successfully describe, employing the same IBM-1 model parameter set, the levels of the stretched ground state band and the quasi γ-band together with those of excited collective 0^+ and 4^+ bands. That indicates the coexistence of different shapes for the ground and excited levels in the γ-unstable deformation region, which is due to the nearness of the deformed-to-spherical phase transition.

It was found that the transition from prolate to oblate deformation, in the case of low-lying collective states, occurs at $A = 194$ for even-even osmium nuclei, and at $A = 192$ for even-even platinum nuclei. A coexistence of prolate ground state and oblate excited states is predicted in the case of ^{184,186}Pt, and ^{188}W.

The evaluation of statistical chaos criteria - the nearest level spacing distribution $P(S)$, has shown that chaoticity slowly increases from the $SU(3)$-limit side, where $P(S)$ has Poisson form. However, in the vicinity of the $E(5) - O(6)$ critical line, chaoticity within isotope chain changes drastically reflecting a complex nature of observed phase transition.

The results of dynamical quantum chaos criteria - the wave function entropy $W^{U(5)}(\Psi_i)$, calculations for the $184 \leq A \leq 194$ region W, Os, and Pt nuclei have shown that the chaoticity with respect to spherical $U(5)$-symmetric basis diminishes towards $E(5) - O(6)$ critical line for each isotope chain. The change is more abrupt in the case of tungsten nuclei, which is explained by the greater stability of prolate axial deformation in the case of

$Z = 74$ tungsten than in the case of $Z = 78$ platinum.

The results of calculations have been compared with the results of other authors obtained in the frameworks of different theoretical approaches. A possibility to compare the results of algebraic complete IBM-1 model with the ones obtained using geometrical rigid triaxial rotator model has been considered.

The studies of nuclear shape phase transitions and their relationship with quantum chaos could be continued also in other directions, e.g.:

a) the study in the frameworks of complete IBM-1 of different shape phase coexistence phenomena, observed in transitional region nuclei at higher excitation energies;

b) the study of phase transitions and quantum chaos employing IBM-2 model, when isospin dependence of nucleons is taken into account;

c) the study of phase transitions in the case of odd and odd-odd nuclei when one observes additional polarization of nuclear core due to interaction with unpaired nucleons.

The results presented in this dissertation have been published in three refereed journal papers [R1,R3,R6], and one paper in international conference proceedings [R5]. One journal paper [R2] has been published in the local scientific journal.

One journal article manuscript [R4], submitted to refereed journal in 2007, presently is revised and extended, including additional calculation results. A journal article manuscript [R7] about results of phase transition and quantum chaos studies for $A \sim 190$ region nuclei is submitted to journal in July, 2010.

The results of studies have been reported both at international and local scientific conferences: eight oral presentations - international [A1,A3,A5,A7,A10], and local [A2,A4,A6], and two poster presentations - international [A8], and local [A9].

Most of the results presented in this doctor dissertation have been obtained as a part of Latvian Science Council research projects No. 05.1707, and No. 09.1194. Also, the financial support of European Social Fund, which gave me a possibility to bring this work to its logical conclusion, is highly appreciated.

I would like to thank all physicists of the LU ISSP Nuclear Reaction Laboratory with whom I have had a pleasure to communicate and work together since 2005, during my Master Course and Doctor Course Studies. I am greatly indebted to former engineers of the Nuclear Reaction Laboratory Mag.Phys. Andrejs Andrejevs and Leonids Neiburgs, as well as two former

LU students: Aleksandrs Dzalbs, and Konstantins Bavrins, for their assistance in some aspects of computer programming and numerical calculations.

Special thanks to my present scientific advisor Dr.phys. Tamara Krasta, who overtook the task to supervise and guide this doctoral work after a sudden demise of my previous teacher and advisor Dr.habil.phys. Juris Tambergs.

And last but not least, I would like to express my love and appreciation to my wife and children for their great patience and understanding, which enables me to devote a considerable part of my time to physics.

Author's list of publications

Journal papers

R1 J. Proskurins, A. Andrejevs, T. Krasta, J. Tambergs. Studies of Phase Transitions and Quantum Chaos Relationships in Extended Casten Triangle of IBM-1. Physics of Atomic Nuclei, 2006, vol.69, p.1248-1253.

R2 A. Andrejevs, T. Krasta, J. Proskurins, J. Tambergs. Precise Solution of the Classical Energy Functional for the Extended Casten Triangle of IBM-1. Latvian J.Phys.Tech.Sci., 2006, No.3, p.58-65.

R3 J. Proskurins, A. Andrejevs, T. Krasta, L. Neiburgs, J. Tambergs. Studies of the Classical Energy Limit of the Interacting Boson Model in the Case of Three-Body Interactions. Bulletin of the Russian Academy of Sciences: Physics, 2007, vol.71, No.6, p.894-900.

R4 J. Proskurins, K. Bavrins, A. Andrejevs, T. Krasta, J. Tambergs. Study of Quantum Chaos in the Framework of Triaxial Rotator Model. Manuscript (10 pages) has been submitted to Physics of Atomic Nuclei in 2007 and presently is in the process of revision.

R5 J. Proskurins, K. Bavrins, A. Andrejevs, T. Krasta, J. Tambergs. Study of quantum chaos in the framework of triaxial rotator models. In: Proc.13th Int. Conf. on Capture Gamma-Ray Spectroscopy and Related Topics. Eds. A. Blazhev, J. Jolie, N. Warr, A. Zilges, AIP Conference Proceedings Vol.1090 (2009), pp.635-636.

R6 J. Proskurins, A. Andrejevs, T. Krasta, J. Tambergs. Phase transitions in the framework of complete version of IBM-1. Bulletin of the Russian Academy of Sciences: Physics, Vol.73, No.2 (2009), pp. 241-244.

R7 J. Proskurins, T. Krasta, K. Bavrins. Study of the onset of chaos in the A 190 nuclear deformation phase transition region. Manuscript (12 pages, September, 2010) submitted for publication in the Bulletin of the Russian Academy of Sciences: Physics.

Conference abstracts

A1 J. Proskurins, A. Andrejevs, T. Krasta, J. Tambergs. Studies of Phase Transitions and Quantum Chaos Relationships in Extended Casten Triangle of IBM-1. In: LV National Conference on Nuclear Physics "Frontiers in the Physics of Nucleus". June 28-July 1, 2005, St.-Petersburg, Russia. Book of Abstracts. St.-Petersburg, 2005, p.95.

A2 J. Proskurins, A. Andrejevs, T. Krasta, L. Neiburgs, J. Tambergs. Studies of Classical Energy Limit of Interacting Boson Model in the Case of Triaxial Deformations. In: LU ISSP 22nd scientific conference, Riga, 29-30 March, 2006. Book of abstracts. Riga, ISSP, 2006, p.27.

A3 J. Proskurins, A. Andrejevs, T. Krasta, L. Neiburgs, J. Tambergs. Studies of Classical Energy Limit of Interacting Boson Model in the Case of Three-Body Interactions. In: 56 International Conference "Nucleus-2006" on Problems of Nuclear Spectroscopy and Structure of Atomic Nucleus, September 4-8, 2006, Sarov, Russia. Abstracts, Sarov 2006, pp.111-112.

A4 J. Proskurins, K. Bavrins, A. Andrejevs, T. Krasta, J. Tambergs. Study of Quantum Chaos in the Framework of Triaxial Rotator Model. In: LU ISSP 23rd scientific conference devoted to the 75th anniversary of LU professor Ilmārs Vītols, Riga, 13-15 February, 2007. Book of abstracts. Riga, ISSP, 2007, p.12.

A5 J. Proskurins, K. Bavrins, A. Andrejevs, T. Krasta, J. Tambergs. Study of Quantum Chaos in the Framework of Triaxial Rotator Model. In: 57 International Conference on Nuclear Physics Nucleus-2007, Fundamental Problems of Nuclear Physics, Atomic Power Engineering and Nuclear Technologies. June 25-29, 2007, Voronezh, Russia. Book of Abstracts, St.-Petersburg, 2007, p.191.

A6 J. Proskurins, K. Bavrins, A. Andrejevs, J. Tambergs. Studies of Phase Transitions and Quantum Chaos in the Framework of Interacting Boson and Geometrical Nuclear Models. In: LU ISSP 24th scientific conference, Riga, 20-22 February, 2008. Book of abstracts. Riga, ISSP, 2008, p.38.

A7 J. Proskurins, A. Andrejevs, T. Krasta, J. Tambergs. Phase Transitions in the Framework of Complete Version of IBM-1. In: 58 International Meeting on Nuclear Spectroscopy and Nuclear Structure "Nucleus-2008". Fundamental Problems of Nuclear Physics, Nuclear Methods in Nanotechnology, Medicine and Nuclear Power Engineering. June 23-27, 2008, Moscow, Russia. Book of Abstracts. St.-Petersburg, 2008, p.165.

A8 J. Proskurins, K. Bavrins, A. Andrejevs, T. Krasta, J. Tambergs. Study of quantum chaos in the framework of triaxial rotator models. In: 13th International Symposium on Capture Gamma-Ray Spectroscopy and Related Topics, Cologne, Germany, August 25-29, 2008. Book of Abstracts, pp.174-175.

A9 J. Proskurins, A. Andrejevs, K. Bavrins, T. Krasta, J. Tambergs. Use of Peres lattice method for the study of nuclear phase transitions. In: LU ISSP 25th scientific conference, Riga, 11-13 February, 2009. Book of abstracts. Riga, ISSP, 2009, p.38.

A10 J. Proskurins, T. Krasta, K. Bavrins. Study of the onset of chaos in the A ~190 nuclear deformation phase transition region. In: "Nucleus 2010. Methods of Nuclear Physics for Femto- and Nanotechnologies (LX Meeting on Nuclear Spectroscopy and Nuclear Structure)", 6-9 July 2010, St.-Petersburg, Russia. Book of Abstracts, St.-Petersburg, 2010, p.214.

References

[1] P. Cejnar, J. Jolie, Progr.Part.Nucl.Phys. **62**, 62 (2009); nucl-th/0807.3467.

[2] Y. Alhassid, A. Novoselsky, N. Whelan, Phys.Rev.Lett. **65**, 2971 (1990).

[3] Y. Alhassid, N. Whelan, Phys.Rev.Lett. **67**, 816 (1991).

[4] P. Cejnar, J.Jolie, Phys.Rev.E. **58**, 387 (1998); Phys.Lett.B **420**, 241 (1998).

[5] P. Cejnar, J. Jolie, Phys.Rev.E **61**, 6237 (2000).

[6] J. Jolie, F.F. Casten, P. von Brentano, V. Werner, Phys.Rev.Lett. **87**, 162501 (2001).

[7] J. Jolie, S. Heinze, A. Linnemann, V. Werner, P. Cejnar, R.F. Casten, in: Proceedings of the 11th International Symposium on Capture Gamma Ray Spectroscopy and Related Topics. Eds. J. Kvasil, P. Cejnar, M. Krtička (World Scientific, Singapore, 2003), p.36.

[8] E. Lopez-Moreno, O. Castanos, Phys.Rev.C. **54**, 2374 (1996).

[9] V.E. Bunakov, in: ISINN-2 Proceedings. Dubna 1994. (JINR, E3-94-419, Dubna, 1994), p.76.

[10] J.M. Eisenberg, W. Greiner. Nuclear Theory. Vol. 1. Nuclear Models. (North-Holland, Amsterdam-London, 1970).

[11] A. Bohr, B. Mottelson, Kgl.Dan.Vid.Selsk., Mat.-Fys. Medd., **27**, No.16, 1 (1953).

[12] A.S. Davydov, G.E. Filippov, Nucl.Phys. **8**, 237 (1958).

[13] V.R. Manfredi, L. Salasnich, Phys.Rev.E **64**, 066201 (2001).

[14] V.R. Manfredi, V. Penna, L. Salasnich, Mod.Phys.Lett.B **17**, 803-812 (2003).

[15] F. Iachello, A. Arima. The Interacting Boson Model. (Cambridge University Press, Cambridge, 1987).

[16] D. Bonatsos. Interacting Boson Models of Nuclear Structure. (Clarendon Press, Oxford, 1988).

[17] O. Scholten, in: Computational Nuclear Physics 1, Nuclear Structure. Eds. K. Langanke, J.A. Maruhn, S.E. Koonin (Springer, Berlin-Heidelberg, 1991), p.88.

[18] R.F. Casten, D.D. Warner, Rev.Mod.Phys. **60**, 389 (1988).

[19] Y. Alhassid, N. Whelan, Phys.Rev.C **43**, 2637 (1991).

[20] J. Jolie, P. Cejnar, R.F. Casten, S. Heinze, A. Linnemann, V. Werner, Phys.Rev.Lett. **89**, 2002, 182502 (2002).

[21] H.-J. Stöckmann. Quantum Chaos. An Introduction. (Cambridge Univ. Press, 2000).

[22] M.V. Berry, M. Tabor, Proc.Roy.Soc.A **356**, 375 (1977).

[23] O. Bohigas, M.J. Giannoni, C. Schmidt, Phys.Rev.Lett. **52**, 1 (1984).

[24] T.A. Brody, J. Flores, J.B. French, P.A. Mello, A. Pandey, S.S.M. Wong, Rev.Mod.Phys. **53** 385 (1981).

[25] V.E. Bunakov, F.F. Valiev, J.M. Chuvilsky, Izv.RAN, ser.fiz. **62**, 41 (1998).

[26] P. Van Isacker, J.-Q. Chen, Phys.Rev.C **24**, 684 (1981).

[27] K. Heyde et al., Phys.Rev.C **29**, 1420 (1984).

[28] G. Thiamova, P. Cejnar, Nucl.Phys.A **765**, 97 (2006).

[29] A.S. Davydov. Excited states of atomic nuclei. (Atomizdat, Moscow, 1967).

[30] A.V. Bravin, A.D. Fedorov, Izv.AN SSSR, ser.fiz. **34**, 454 (1970).

[31] A.D. Fedorov, Yadernaya fizika (Sov.Journal of Nucl.Phys.) **15**, 36 (1972).

[32] NNDC On-Line Data Service from ENSDF database, http://www.nndc.bnl.gov/ensdf/.

[33] J. Jolie, A. Linnemann, Phys.Rev. C, **68** (2003) 031301.

[34] J.M. Arias, et al., Phys.Rev.C. **68**, 041302, (2003).

[35] F. Iachello, Phys.Rev.Lett. **87**, 052502 (2001).

[36] F. Iachello, Phys.Rev.Lett. **85**, 3580 (2000).

[37] Liao Ji-zhi, Wang Huang-sheng, Phys.Rev.C **49**, 2465 (1994).

[38] V.R. Manfredi, V. Salasnich, Int.J.Mod.Phys.E **4**, 625 (1995).

[39] P.D. Stevenson et al., Phys.Rev.C **72**, 047303 (2005).